5-2014

Use of Alkali Metal Salts to Prepare High Purity Single-Walled Carbon Nanotube Solutions and Thin Films

Rakan F. Ashour

USE OF ALKALI METAL SALTS TO PREPARE HIGH PURITY SINGLE-WALLED CARBON NANOTUBE SOLUTIONS AND THIN FILMS

Rakan F. Ashour

B.S. Mechanical Aerospace Engineering, King Abdulaziz University,

Jeddah, Saudi Arabia

A thesis submitted in partial fulfillment of the

requirements for the degree of

Master of Science in Materials Science and Engineering in the

School of Chemistry and Materials Science,

College of Science

Rochester Institute of Technology

May 2014

Signature of the Author _____

Accepted by _____

Director, M.S. Degree Program Date

SCHOOL OF CHEMISTRY AND MATERIALS SCIENCE
COLLEGE OF SCIENCE
ROCHESTER INSTITUTE OF TECHNOLOGY
ROCHESTER, NEW YORK

CERTIFICATE OF APPROVAL

M.S. DEGREE THESIS

The M.S. Degree Thesis of Rakan F. Ashour has
been examined and approved by the thesis
committee as satisfactory for the thesis required for
the M.S. degree in Materials Science and Engineering.

_____

Dr. John-David R. Rocha, *Thesis Advisor*

_____

Dr. Christopher J. Collison, Committee Member

_____

Dr. Michael S. Pierce, Committee Member

_____

Dr. Thomas W. Smith, Committee Member

_____

Date

ABSTRACT

Single-walled carbon nanotubes (SWCNTs) display interesting electronic and optical properties desired for many advanced thin film applications, such as transparent conductive electrodes or thin-film transistors. Large-scale production of SWCNTs generally results in polydispersed mixtures of nanotube structures. Since SWCNT electronic character (conducting or semiconducting nature) depends on the nanotube structure, application performance is being held back by this inability to discretely control SWCNT synthesis. Although a number of post-production techniques are able to separate SWCNTs based on electronic character, diameter, or chirality, most still suffer from the disadvantage of high costs of materials, equipment, or labor intensity to be relevant for large-scale production. On the other hand, chromatographic separation has emerged as a method that is compatible with large scale separation of metallic and semiconducting SWCNTs.

In this work, SWCNTs, in an aqueous surfactant suspension of sodium dodecyl sulfate (SDS), are separated by their electronic character using a gel chromatography process. Metallic SWCNTs (m-SWCNTs) are collected as initial fractions since they show minimum interaction with the gel medium, whereas, semiconducting SWCNTs (sc-SWCNTs) remain adsorbed to the gel. The process of sc-SWCNT retention in the gel is found to be driven by the packing density of SDS around the SWCNTs. Through a series of separation experiments, it is shown that sc-SWCNTs can be eluted from the gel simply by disturbing the configuration of the SDS/SWCNT micellar structure. This is achieved by either introducing a solution containing a co-surfactant, such as sodium cholate (SC), or solutions of alkali metal ionic salts. Analysis of SWCNT suspensions by optical

absorption provides insights into the effect of changing the metal ion (M^+ = Li^+, Na^+, and K^+) in the eluting solution. Salts with smaller metal ions (e.g. Li^+) require higher concentrations to achieve separation. By using salts with different anionic groups (cholate, Cl^-, I^-, and SCN^-), it is concluded that the SWCNT separation using salt solutions is mainly driven by the cations in the solution.

Additionally, different methods for depositing separated SWCNTs on glass substrates are described. In one method, SWCNTs are first isolated from their surfactant by introducing organic solvents such as methanol or acetone to aqueous suspensions of previously separated m- and/or sc-SWCNTs. Following the induced SWCNT dissolution, desired nanomaterials can be redispersed directly in another solvent, such as methanol, for deposition on substrates. In another method, separated SWCNTs are deposited on glass substrates by the process of evaporation driven self-assembly. Different morphologies on the substrate are formed by changing the viscosity of the evaporating SWCNT/SDS suspensions. The results are described using the Stokes-Einstein equation for diffusion in one dimension.

DEDICATION

To my wife Jomana for standing by my side through my degree and supporting me with her love and compassion, and my daughter Ayah for putting a smile on my face every time I'm faced with a stressful situation.

To the greatest parents in the world; Faeyg Ashour and Eman Alawi, you have been the best role models any person could ask for and I'm truly blessed to have been raised by you.

To my little brother Mansour.

ACKNOWLEDGMENTS

First and foremost, I would like to thank my advisor Dr. John-David R. Rocha for taking me in his group knowing that I come from a completely different academic background. I truly admire his passion for research and his desire to help everyone. I'm very thankful for all the opportunities that he provided for me and the rest of the NanoMaterials Spectroscopy Lab group.

I would like to thank my committee members: Dr. Christopher Collison, Dr. Michael Pierce, and Dr. Thomas Smith for their professional guidance and valuable input on all parts of this thesis.

Members of the NanoMaterials Spectroscopy Lab: Leonard Breindel, Ryan Capasse, Alyssa Dibble, Mikhail Solomonik, and Dustin Woods. Thank you for the valuable discussions and friendship. In particular, I would like to acknowledge Leonard Breindel who is a great scientist in the lab and a true friend outside.

TABLE OF CONTENTS

LIST OF FIGURES

LIST OF TABLES

CHAPTER 1: INTRODUCTION

1.1 Structure of Single-walled Carbon Nanotubes

A theoretical description of the structure of single-walled carbon nanotubes arises from its closely related two dimensional graphene. A single-walled carbon nanotube can be thought of as a single layer of graphene rolled up to form a tube. Depending on the direction at which this sheet is rolled a wide range of tubular shapes can be generated. The generated shapes are differentiated by their chirality and diameter (Figure 1.1).

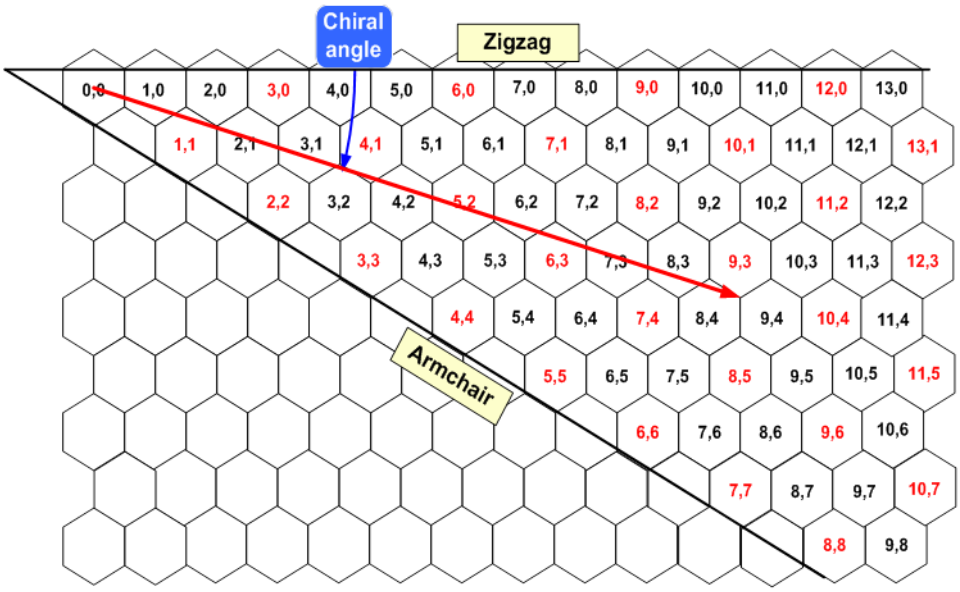

Figure 1.1 Chiral vector representation of SWCNT structure.

The structure of a single-walled carbon nanotube is specified by what is known as the chiral vector. This vector describes how the tubular structure is formed from the flat graphene sheet. The mathematical expression for the chiral vector **C** takes into account the vectors of the graphene lattice $\mathbf{a}_1$ and $\mathbf{a}_2$ which form an angle of 30° on the graphene sheet.[1] Since the formation of a tube includes a finite number of hexagonal unit cells along the circumference, the two integers *n* and *m* are introduced to account for the number of hexagonal cells along the vectors $\mathbf{a_1}$ and $\mathbf{a_2}$ respectively (Equation 1.1).

$$\mathbf{C} = n\,\mathbf{a_1} + m\,\mathbf{a_2} \qquad (1.1)$$

The direction of the chiral vector **C** is perpendicular to the axis of the tube formed and the length of the vector corresponds to the circumference of the tube. The diameter and chiral angle can also be determined using the vector **C** as shown in equations (1.2) and (1.3):

$$D = \frac{|\mathbf{C}|}{\pi} = \frac{a_0}{\pi} \times \sqrt{n^2 + n \cdot m + m^2} \qquad (1.2)$$

$$\theta = \frac{\cos^{-1}(\mathbf{a_1}.\mathbf{C})}{|\mathbf{a_1}||\mathbf{C}|} \qquad (1.3)$$

where a_0 is the C-C bond distance. In the example shown in Figure 1.1, the chiral vector is $\mathbf{C} = 9\,\mathbf{a_1} + 4\,\mathbf{a_2}$ or it is referred to as a (9,4) nanotube. Using equation (1.2) with a_0 = 0.146 nm gives a diameter of 0.9 nm for this nanotube and a chiral angle of 17.4°. Accordingly, the structure of any single-walled carbon nanotube can be described by the two integers (*n*,*m*).

From a symmetry point of view, all SWCNTs are categorized as either being chiral or achiral. In the case of an achiral nanotube the mirror image is considered to be super-imposable on the original structure (Figure 1.2a&b). On the other hand in a chiral nanotube the mirror image of the SWCNT is different from its original structure (Figure 1.2C).

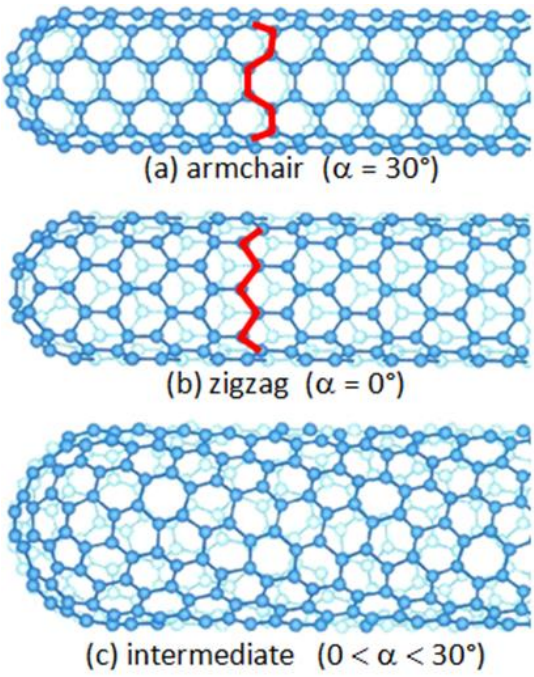

Figure 1.2 Different structures for a single-walled carbon nanotube. (a) armchair, (b) zigzag and (c) chiral.

The majority of SWCNTs with (*n*,*m*) are considered chiral meaning they possess left or right handedness. In the case when $m = 0$, the nanotube has a chiral angle of 0° and such nanotubes are called zigzag, which refers to the arrangement of the hexagonal cell on the surface of the nanotube. In another case when $n = m$, the chiral angle is 30^0 and the nanotubes are called armchair. In both cases, the nanotubes are achiral and possess a super-imposable mirror image. The characteristic structural parameters for the armchair, zigzag and chiral nanotubes are summarized in Table 1.1.

Table 1.1 Summary of characteristic structural parameters for the three classes of SWCNTs. Adopted and modified from reference 1.

	Description	Diameter	Chiral Angle
Armchair	(*n*,*n*)	$\sqrt{3}\,\frac{n\,a_0}{\pi}$	30°
Zigzag	(*n*,0)	$\frac{n\,a_0}{\pi}$	0°
Chiral	(*n*,*m*)	$\sqrt{n^2+nm+m^2}\,\frac{a_0}{\pi}$	$\frac{cos^{-1}(n+\frac{m}{2})}{\sqrt{n^2+nm+m^2}}$

There are two main types of bonds in a carbon nanotube. One is the sigma (σ) bond along the axis of the nanotubes giving them mechanical strength and making them one of the strongest materials known to mankind. The other type of bond is the pi (π) bonds which form perpendicular to the axis of the nanotubes. The electronic character of a carbon nanotube is governed by the perpendicular π bonds since they can cross the Fermi level and form bonding and anti-bonding orbitals which in turn determine if the carbon nanotube is metallic or semiconducting.

The details of the theoretical derivation of the electronic band structure will not be presented in this thesis since that has already been described in a large number of textbooks and papers.[1-4] However, the results of the theoretical work is of great importance to this work as it relates the electronic character of a SWCNT to both the diameter and (*n*,*m*) structure.

The electronic band structure of a SWCNT is derived from that of graphene by applying the zone folding approximation.[5] The band structure of graphene is determined using a quantum mechanical model termed “tight binding”. Electrons are free to move in

the graphene sheet since the valence and conduction bands meet at several points in the energy domain. The same points are observed in metallic SWCNTs due to the existence of a number of electronic states connecting the valence and conduction band. When no electronic states are present between the two bands, an energy gap forms making the SWCNT behave as a semiconductor.

Due to the geometry of a SWCNT, a mixing of π and σ orbitals occurs which leads to a shift in the allowed energy bands from the graphene. Larger diameter SWCNTs are expected to have an electronic character similar to that of graphene. On the other hand, smaller diameters are expected to have a wide band gap. Additionally, using the relation:

$$\frac{(n-m)}{3} = p \qquad (1.5)$$

one can classify SWCNTs as metallic or semiconducting. If p is an integer then the nanotube is metallic, otherwise the nanotube behaves as a semiconductor. Therefore we can generalize that all armchair nanotubes with (n,n) are metallic as the relation in (1.5) gives an integer every time. For the zigzag (n,0), the nanotubes are metallic when n is a multiple of 3, such as (3,0) or (15,0), and otherwise a semiconductor, as in (4,0) or (13,0). Additionally, equation (1.5) indicates that one third of possible SWCNT species are considered metallic while two thirds are considered semiconducting.

1.2 Synthesis of single-walled carbon nanotubes

A general approach in synthesizing carbon nanotubes in the form of either multi, double of even single-walled structures requires a carbon source, a catalyst and an energy input. The most commonly used techniques to produce SWCNTs include catalytic chemical vapor deposition (CCVD), arc discharge, and pulsed laser deposition.[6-8]

In CCVD a carbon containing source in a gas or liquid form is fed into a chamber holding the catalyst particles at elevated temperatures. A large amount of work is put into studying the effect of changing different synthesis parameter conditions on the produced nanotubes samples. CVD techniques include high pressure CO decomposition (HiPco), cobalt molybdenum catalyst (CoMoCAT), plasma enhanced chemical vapor deposition (PECVD) and laser assisted chemical vapor deposition (LCVD). The wide range of developed techniques makes CVD the most common route by which carbon nanotubes can be produced, as well as, being the most suitable for large industrial scale production.

During growth, process catalyst particles can be either floating, or deposited on a substrate (supported catalyst). Currently, the method of floating catalyst is used to produce high purity commercial quantities of single-walled carbon nanotubes using a HiPco process developed by the Smalley group at Rice University.[8] The catalyst is fed into the chamber by decomposing a metal-based compound to a gaseous state that can be entrained in an inert carrier gas (e.g. nitrogen or argon). In the same manner carbon is introduced via the decomposition of carbon containing compounds. Clusters of carbon and catalyst particles form once they are in vapor form. Although different descriptions of the mechanism by which nanotubes grow were proposed, the model proposed by Dai et.al [8] introduced the idea of cap formation as a necessary step in the growth of carbon nanotubes. Later, Fan et.al[9] supported this concept by using density functional theory calculations to demonstrate that the formation of a cap is the most favorable energy route. After the cap is formed on the catalyst, further addition of carbon atoms results in the growth of carbon nanotubes. This means that if more than one cap is formed on a single catalyst it's possible to grow many nanotubes on the same catalyst.

Floating catalysts are also applicable in arc discharge and laser vaporization to produce single and multi-walled carbon nanotubes. An example of the floating catalyst technique is the HiPco process in which the produced SWCNTs typically have a range of diameters between 0.8 to 1.4 nm and contain approximately 30 different (*n*,*m*) species.[6]

In the case of a supported catalyst, the process is more complicated since the interaction between catalyst and substrate particles is still a topic of investigation.[10] The basic steps of CVD growth still apply to the supported catalyst method. That is, an initial formation of a cap is essential for the growth of a nanotube. During the growth, the catalyst particles either remain on the substrate or detach from the surface of the substrate. An example of a technology that exploits supported transition metal catalysts is the CoMoCAT process developed by Resasco's group at the University of Oklahoma and subsequently commercialized by Southwest NanoTechnologies, Inc. (SWeNT).[11]

In this technique CoMo bimetallic catalyst particles are embedded in silica based substrates. The process starts by first heating the supported catalyst to a high temperature, between 600 – 900 ^{o}C. If single-walled carbon nanotubes are desired then CO is introduced as the carbon source. However, if multi-walled nanotubes are desired then C_2H_4 is used.[7] In the case of SWCNTs, the range of diameters that this method yields is similar to that of the HiPco process, between 0.8 and 1.2 nm. However unlike HiPCO, there are only approximately 5 to 20 (*n*,*m*) species present with (6,5) being the dominating chirality with a percentage of more than 40%. This composition was observed when the fluorescence map of both CoMoCAT and HiPco SWCNTs suspended in solution were presented by the Weisman group at Rice University (Figure 1.3).[6]

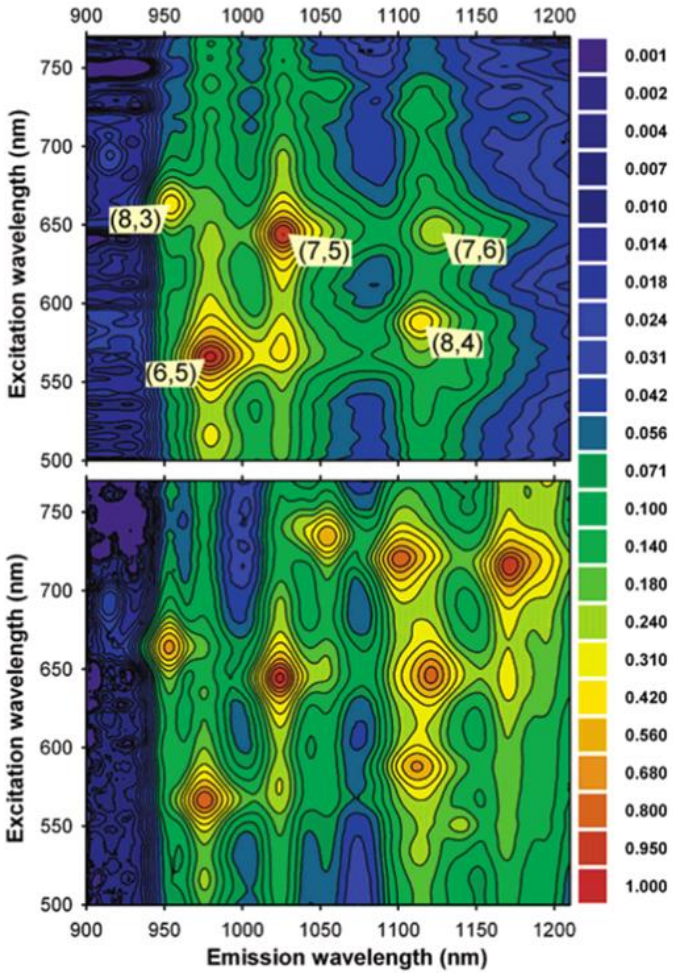

Figure 1.3 – Comparative fluorescence maps of SWCNTs produced via the CoMoCAT process (top) versus those produced by the HiPco method (bottom). Adopted from reference 6.

For all production methods to date, the produced SWCNT samples have a range of diameters and chiralities. This is believed to be the result of having catalyst particles with different sizes, but the role of catalyst particles in the synthesis process is not limited to being nucleation sites; it also dictates the diameter of the carbon nanotubes growing on them. Ongoing research in the field is considering different approaches to control the size of the catalyst particles as well as their crystal structure and eventually hope to obtain more control over the diameter and chirality of produced samples.

1.3 Applications of SWCNTs

A couple of decades after the first purposeful observation of hollow nanometer sized carbon structures by Ijima,[12] carbon nanotubes are still one of the most widely investigated materials around the world. Researchers from many different disciplines are studying the properties of SWCNTs. Mechanical and aerospace engineers for example are interested in the exceptional strength observed by the material, where experimental work has demonstrated an ultimate tensile strength of 50 GPa.[13,14] The attractive feature of SWCNT to mechanical applications is the low density which can allow structures combining high strength and low weight. The application of SWCNTs into mechanical structures is usually done by considering them as the reinforcing agent in polymer/SWCNT composites.

The conductivity of SWCNTs differs depending on the diameter and chirality (as previously described). Metallic SWCNTs display extraordinary conductivity which is desired in advanced applications such as conductive thin films.[15] Another emerging application which depends on the conductivity of SWCNTs is printable super-capacitors in which SWCNTs are used as the charge collector and the electrode.[16] Semiconducting nanotubes on the other hand are considered for applications such as organic field effect transistors (OFET)[17,18] since they display very high carrier mobility compared to conventional silicon. The sensitivity of SWCNTs to the surrounding environment qualifies them for many biological sensing applications where they can be applied as a chemo-resistive layer in a sensor. Biological molecules can form non-covalent bonds with the surface of the nanotube which then causes a change in electrical conductance. More recently, emerging optoelectronic applications are taking advantage of the

interesting properties of SWCNTs to produce energy harnessing devices.[19,20] There are many ways that one can apply nanotubes in photoconductive devices. SWCNTs can be used to fabricate transparent conductive anodes which can be used as an alternative to indium tin oxide (ITO). Another possible route is to use SWCNT in the active layer of bulk heterojunction organic solar cells.[21]

1.4 Obstacles of SWCNTs characterization and applications

The structure and size of SWCNTs are the attractive features that make them ideal for many applications. Most applications that are described in the previous section require knowledge of the diameter and chirality of the nanotubes used. In the case of mechanical structures, for instance, the strengthening mechanism cannot be fully exploited if more than one diameter is present since the interface between SWCNTs/matrix is believed to be diameter dependent. Moreover, in applications such as nano-electronics, the presence of many different chiralities can greatly impact the overall properties of the material. In the case of photoconductive transducers, when more than one chirality is used in a device, the interaction between nanotubes with different band gaps can result in performance degradation.[19,20]

Although the solution to these problems might seem straightforward, it's still not possible to synthesize SWCNTs with a desired diameter and chirality due to the difficulties of controlling catalyst size. Therefore all available synthesis methods produce SWCNTs with a range of diameters and chiralities. Furthermore, produced carbon nanotubes are usually accompanied with catalyst particles as well as carbonaceous impurities. This requires post-production treatment, which is usually done using chemical

treatments like harsh acid digestion where imperfections to SWCNT structures or changes in their properties can be induced.

While researchers are showing progress in the field of selective growth, many have turned their attention to post-production separation. Currently, SWCNTs are isolated based on diameter, electronic character, and chirality. More details on post-production separation are presented in the next section.

The second most challenging factor that has been holding back many advanced applications of SWCNTs is the ability to characterize the produced samples in an efficient and accurate way on a large scale. Early efforts used high resolution electron microscopy or scanning tunneling microscopy to measure different diameters and identify different chiralities.[22] However, the method is only applicable to research scale and is also considered very expensive considering the cost of the instruments needed.

The most recent technique exploits the dependence of the energy band gap on the (*n,m*) indices and the ability of SWCNTs to fluoresce for identifying and quantifying different diameters and chiralities.[23-25] However this technique can only be applied to identify semiconducting SWCNTs. In addition, conventional fluorescence experiments are considered time consuming and not compatible with large scale characterization. Another simple and convenient method is absorption spectroscopy which can be applied to identify both metallic and semiconducting SWCNTs generally by their diameter and chirality. The method allows the observation of many allowed electronic transitions in semiconducting SWCNTs such as the S_{11} (850 – 1400 nm) and S_{22} (450 – 750 nm) which refer to the first and the second allowed electronic transitions respectively. Moreover, it also allows for the detection of electronic transitions that take place in metallic SWCNTs,

namely M_{11} which is typically observed in the near ultra-violet region (300 – 450 nm).[26,27]

1.5 Overview of post-production separation methods

The need for separation techniques has been driven by the inability of current techniques to synthesize a single electronic type or diameter. Although research in the field is still active, trying to control the diameter of a catalyst nanoparticle to a precision of a few angstroms, the difference between (*n*,*m*) types, is very difficult. Moreover, even if large scale diameter control was made possible, the prospect of having different chiralities with the same diameter still exists. Therefore, development of an efficient and cost effective post-production separation method is of great importance.

There are different techniques by which a separation of SWCNTs based on diameter, chirality and electronic character can be achieved. These techniques can be classified into two main categories: one is physical methods which include electrophoresis and density gradient ultracentrifugation (DGU).[28-30] The other category is separation by chemical methods which involves selective covalent or non-covalent functionalization of the nanotube surface.[31,32] The common factor between all currently used techniques is the necessity to suspend SWCNTs into a solution to be able to separate them.

1.5.1 Electrophoresis separation

Electrophoresis is used to separate carbon nanotubes produced by different synthesis techniques into metallic and semiconducting fractions.[19] The method uses two charged electrodes in a solution of suspended SWCNTs. The electric field from the electrodes creates a dipole in each nanotube with magnitude proportional to the dielectric

constant of the nanotube. Since the m-SWCNTs have a dielectric constant that is much greater than that of a sc-SWCNT, metallic species align in the direction of the field and move toward the charged electrodes (Figure 1.4, left). This results in having separated and aligned metallic nanotubes on the electrodes.

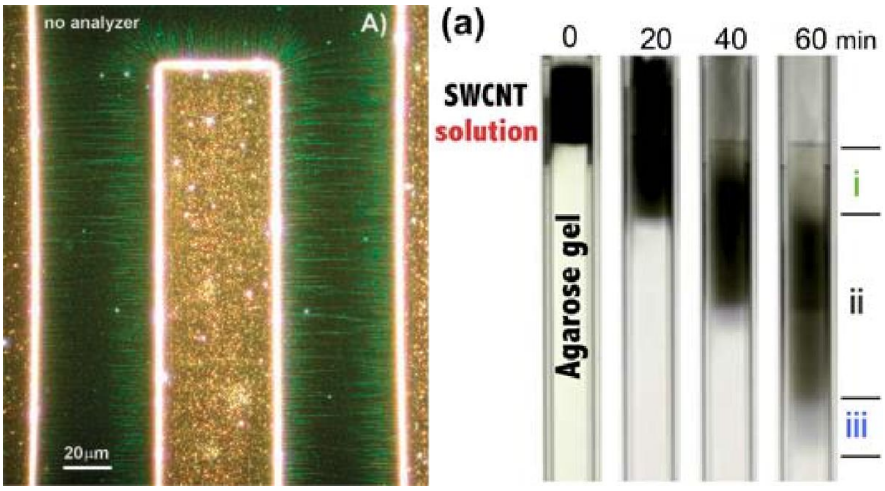

Figure 1.4 – (left) Example of aligned metallic SWCNTs across electrode channels of a dielectrophoretic separation system,[33] (right) example of separated metallic (*iii*) and semiconducting (*i*) SWCNTs during a gel electrophoresis experiment.[34]

Besides sorting, the main advantage of electrophoresis is the alignment of separated samples, however this method suffers from low material outputs making it non-ideal for large scale separations. It is also possible to apply the electric field across a gel (as used for DNA or other biological molecules) to affect a separation (Figure 1.4, right).

1.5.2 Density Gradient Ultracentrifugation

Another promising technique is density gradient ultracentrifugation (DGU) developed by Hersam's group from Northwestern University.[30] This method exploits the slight difference in density between different nanotubes, and the technique has been used in biochemistry for a period of time to separate micro-molecules based on their densities before applying it to carbon nanotubes.[35] DGU separation experiments start by loading suspended SWCNTs, typically by a surfactant or ss-DNA, into an aqueous solution of

iodixanol with known density gradient. When a centrifugal force (generally > 100,000×g) is applied, nanotubes with certain diameter move toward the region where their density matches that of the gradient (Figure 1.5).

DGU also exploits the difference in packing density of a surfactant micellar structure around nanotubes with different diameters. Surfactants such as sodium dodecyl sulfate (SDS) will have a higher packing density with metallic nanotubes. Therefore, the supramolecular structure of SDS/SWCNT will have a higher density and consequently will be forced to move further down toward the high density medium.[36] However, DGU experiments which use a mixture of surfactants indicate that the position of metallic and semiconducting SWCNTs can be affected by the choice of the main dispersing surfactant and the co-surfactant.

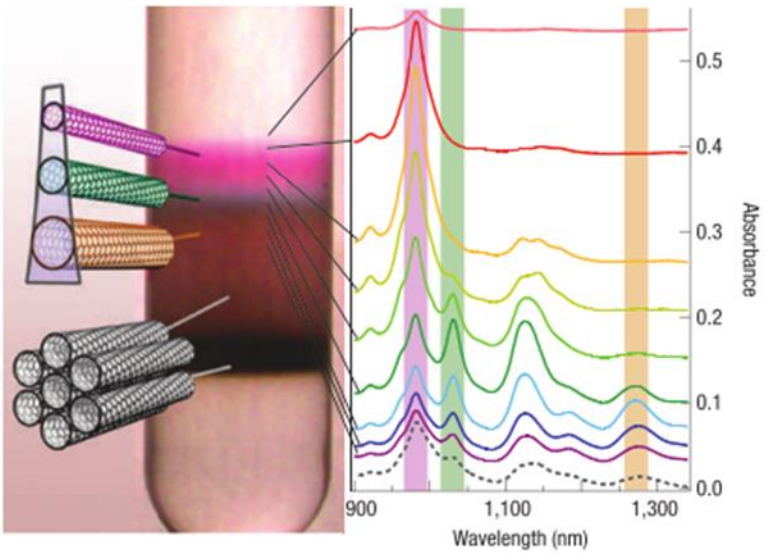

Figure 1.5 CoMoCAT SWCNT/SC separated using density gradient (adopted from reference 30).

In the work of Kataura's group,[37,38] when SDS is used as the main surfactant and sodium cholate (SC) as a cosurfactant, metallic nanotubes are found to have lower density. The mechanism can be described in terms of adsorption of co-surfactant to SWCNTs that are partially covered with main surfactant micelles. In the case of SDS

being the main surfactant, smaller diameter nanotubes will have more exposed regions due to the energetics of SDS wrapping which favor larger diameter SWCNTs.[39] This allows more cosurfactant molecules to adsorb leading to an overall increase in the density of smaller diameter SWCNT/surfactant. [36,40]

Even though DGU is claimed to be compatible with large industrial scale separation, it suffers from the disadvantage of high costs since it employs iodixanol or similar reagents to create a density gradient medium in addition to the high cost of the instruments involved. Moreover, DGU is found to give low yields, as identified from the height of absorption peaks at wavelengths corresponding to most abundant (*n*,*m*) species in a sample, as well as, requiring special fractionation techniques to extract the separated SWCNTs from the iodixanol.

1.5.3 Chromatography Separation

The most promising sorting technique to date that should be suitable for large-scale production is gel chromatography. The technique was employed by the two groups of Moshammer et al.[41] and Katuara et al.[37] The process involves sonication of SWCNTs in the presence of a low concentration of SDS surfactant (0.5% - 3%). The suspended SWCNTs are then loaded onto a column packed with a hydrogel (Sephacryl or agarose). Upon loading, sc-SWCNTs are retained in the column, while m-SWCNTs pass through the medium showing minimal to no interaction (Figure 1.6). This allows for immediate collection of metallic SWCNTs. The retained semiconducting SWCNTs can be released from the gel medium by the introduction of a cosurfactant or solution of high concentration of the same surfactant.[37]

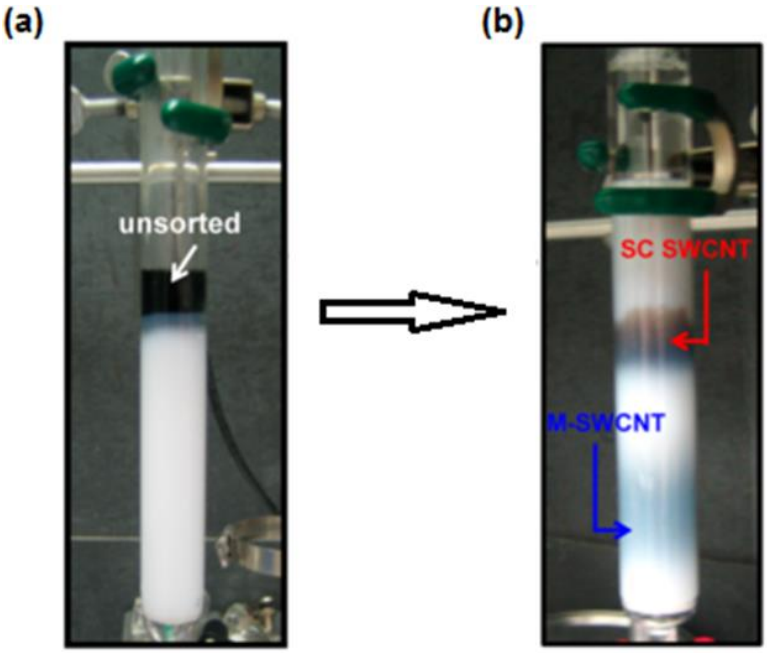

Figure 1.6 SWCNT separation using gel chromatography. (a) initial loading (b) retention of semiconducting SWCNTs. Adopted and modified from reference [42].

The first attempt to describe the mechanism responsible for the separation was made by Moshammer et al.[41], where a proposed size exclusion mechanism was hypothesized. In the same work, the authors proposed that the retention of semiconducting species is mainly due to the formation of bundles of sc-SWCNTs in the gel medium. Those bundles are described to have larger size than the pore size of the filtration medium. Metallic nanotubes are described to be more individualized in their surrounding micelle structure and therefore do not form bundles, which leads to their elution.

The process was then described as selective adsorption by Kataura et al.,[37] in which SWCNTs with different electronic character tend to react in a different way toward the gel medium. In other words, SWCNTs with different electronic characters will have different reaction rates. Many different approaches have been developed based on the selective adsorption explanation.[43-45]

A modified approach that allows separation and isolation of a narrow range of semiconducting SWCNTs was developed by Kataura et al.[44] This method exploits the difference in affinity of different (*n,m*) sc-SWCNTs to a specific functionality type prevalent on the Sephacryl medium. By overloading a gel medium with a large amount of unsorted SWCNT/SDS solution, SWCNTs with highest affinity will be the first to adsorb to the gel followed by the next highest affinity. Therefore by overloading a column with volume ratio of 8:1 of SWCNTs to gel, a narrow range of chiralities are adsorbed in the gel. The method is also extended to include multiple columns connected in series.[44] The results demonstrate that smaller diameter semiconducting SWCNTs display higher affinity towards the gel than those of larger diameter.

In an attempt to understand the process of single chirality separation, a kinetic model was developed by Strano's research group.[46] In their paper the authors assumed a finite number of binding sites that can bind to an (*n,m*) SWCNT. Also, the authors assumed that binding occurred between SWCNTs and the secondary amide group on the polymer. Based on their assumption they have been able to calculate the binding rate constant for different (*n,m)* chiralities. However, the proposed model does not take into account the difference of surfactant arrangement around different nanotubes and assumes the adsorption of exposed regions of semiconducting SWCNTs.

Despite the advancement of chromatography as an ideal mechanism to separate metallic and semiconducting SWCNTs, the driving mechanism is still not fully understood. Recently, a description of the separation process by Hirano et.al [45] provided a thermodynamical insight on the mechanism driving the separation. The proposed model uses a Langmuir isotherm to calculate adsorption rate constant for metallic and

semiconducting SWCNTs. The method is commonly applied to describe the adsorption of gas molecules on a certain substrate. In the case of SWCNTs, the assumption remains that a finite number of adsorption sites exist on the gel and each can only be occupied by a single SWCNT. Therefore the reaction of either a metallic or a semiconducting SWCNT can be described by the following relations

$$\theta = \frac{Kc}{1 + Kc} \tag{1.6}$$

$$c = c_o - \theta\alpha\frac{V_{gel}}{V_{sol}} \tag{1.7}$$

Where c is the final concentration of unadsorbed SWCNT, c_o is the initial concentration, α is the saturation adsorbed SWCNT per unit volume, K is the equilibrium constant, V_{gel} and V_{sol} are the volume of the gel and the aqueous solution respectively. Combining both equations (1.6 and 1.7) gives the relation

$$\frac{V_{gel}\, c}{V_{sol}\,(c_o - c)} = \frac{1}{\alpha K} + \frac{c}{\alpha} \tag{1.8}$$

The left hand side of equation 1.8 can be determined experimentally and plotted versus the unadsorbed SWCNT concentration, thus allowing for the extraction of the saturation factor and equilibrium constant from the slope and intercept, respectively. In this case, Hirano deduced that the rate of reaction of semiconducting SWCNTs is much higher than that of metallic SWCNTs proving the initial hypothesis of selective adsorption. It is important to note that the adsorption is assumed to be between SWCNT/SDS and the gel.

The rate constant is then used to determine the enthalpy of the reaction using the van't Hoff equation, which relates the change in the heat of reaction to the change in rate constant at different temperatures. Since the change in the enthalpy is found to be

positive, the reaction is endothermic. In other words, the reaction needs heat for it to initiate.

From a thermodynamic point of view, in order for any reaction to occur, the total change in free energy has to be negative. This is described using the standard Gibbs free energy formula in equation 1.9,

$$\Delta G = \Delta H - T\Delta S \qquad (1.9)$$

According to equation 1.9, if the reaction is determined to be endothermic in nature (i.e. ΔH is positive), then the second term has to be negative in order for the reaction to occur. The increase in the disorder of the system might be the result of the movement of SDS monomers around SWCNTs when coming in close contact to the binding site on the gel. This description makes it possible to determine the effect of changing the temperature on the adsorption of SWCNTs.

In the recent work of Kataura et.al,[47] they demonstrate the ability to effectively separate SWCNT solutions to achieve enrichment in a few (*n*,*m*) chiralities by changing the temperature of the gel medium. The work demonstrates the dependence of adsorption strength of some (*n*,*m*) chiralities on the surrounding temperature. Lowering the temperature has shown to selectively reduce the strength of adsorption of larger diameter semiconducting nanotubes. Based on their findings they proposed a large scale single chirality separation technique by using a series of columns with different temperatures (Figure 1.7).

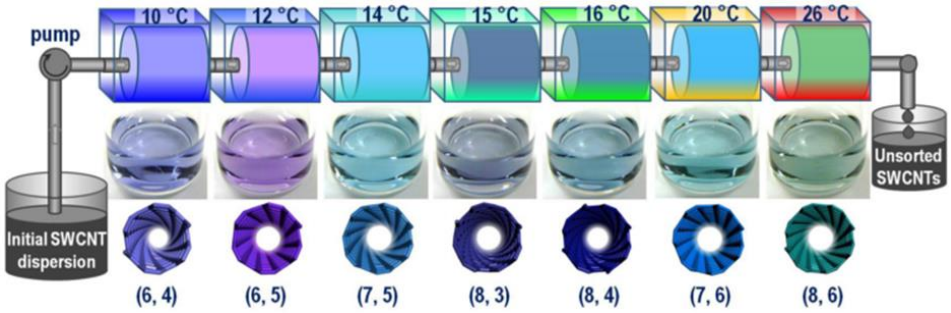

Figure 1.7 Temperature controlled single chirality enriched separation. Adopted and modified from reference [47].

Although the method yields an effective enrichment of a single (*n,m*) species, it does not take into account the effect of surfactant orientation around SWCNTs with different diameters and chiralities. In addition it excludes the effect of temperature on the critical micelle concentration of SDS around SWCNTs.

1.6 Research Directions

This thesis will explore two areas relevant to the large-scale application of SWCNTs. Chapter 2 will be focused on improvements in the gel-based chromatographic separation of SWCNTs. Efforts to reduce sample preparation procedures and complexity will be discussed as well as a broadened study of positive electronic type separations and their influence by the addition of various alkali metal salts. In Chapter 3, the focus is on methods for simplifying the production of SWCNT thin films for future studies in areas like nanoelectronics or imaging. The addition of simple organics like methanol or acetone can assist in removal of surfactants undesired in deposited SWCNT thin films. Furthermore, the use of direct evaporative deposition of SWCNT/surfactant complexes from aqueous suspensions is shown to yield micron to millimeter scale ordering that is controllable via temperature, surfactant concentration, and salt addition.

CHAPTER 2: ELECTRONIC SEPARATION OF SINGLE-WALLED CARBON NANOTUBES

2.1 Single-walled Carbon Nanotube Solutions

Many properties of SWCNTs such as optical absorption, fluorescence and charge transfer can be better understood after separating the tubes in solution. The challenge of solubilizing SWCNTs lies in the nanometer radial dimensions of the material along with very high aspect ratio; the length of a nanotube can be as long as a few centimeters where its diameter can be of a few nanometers. The obstacle here is overcoming van der-Waals forces which increase for nanotubes with larger surface area.

Early work employed organic solvents to solubilize SWCNTs.[48,49] In the work by Haddon et al.[50] carbon nanotubes are dispersed in different organic solvents such as benzene and chloroform. The solubility in organic solvents was described systematically by Cheng et.al using Hansen parameters.[48] The use of organic solvent can be beneficial in some applications such as mechanical reinforcement. However, for applications such as biological sensors, organic solvents can be less tolerable. Therefore a need for SWCNT solubilization in an aqueous medium has driven the development of an alternative approach. The mechanism of suspending SWCNTs in an aqueous solution is based on the ability of amphiphilic molecules (surfactants) to adsorb on the surface of a SWCNT. A simple description of a surfactant is a molecule which has both a hydrophilic head group and a hydrophobic tail group.

Surfactants can be classified depending on the charge on their hydrophilic heads. Surfactants with negative head groups are called anionic surfactants. Examples of anionic surfactants used to prepare SWCNT solutions are sodium dodecyl sulfate (SDS), sodium

dodecyl benzenesulfonate (SDBS), sodium deoxycholate (SDOC), and sodium cholate (SC).[51,52]

The use of surfactants is considered to be the most common technique, to date, that can be used to make stable suspensions of carbon nanotubes. The understanding of SWCNT/surfactant suspensions stems from the non-covalent chemistry of the surface of the nanotubes. The description of the process was proposed by Strano et al.[53] Initially, carbon nanotubes are produced in bundles due to strong van der Waals forces between the SWCNTs. Therefore, initial energy input is required to break these forces. This is commonly done by sonication which provides sheer forces that are able to loosen the ends of bundled nanotubes (Figure 2.1a). Since the carbon nanotubes are hydrophobic in nature, the hydrophobic surfactant tails can then adsorb to the loose ends and prevent them from re-bundling (Figure 2.1b). As the sonication continues to provide sheer that gradually releases the bundled SWCNTs, surfactant molecules continue to adsorb onto the surface. Eventually, surfactant molecules form micelle structures on the surface of each SWCNT leading to their suspension (Figure 2.1d).[29]

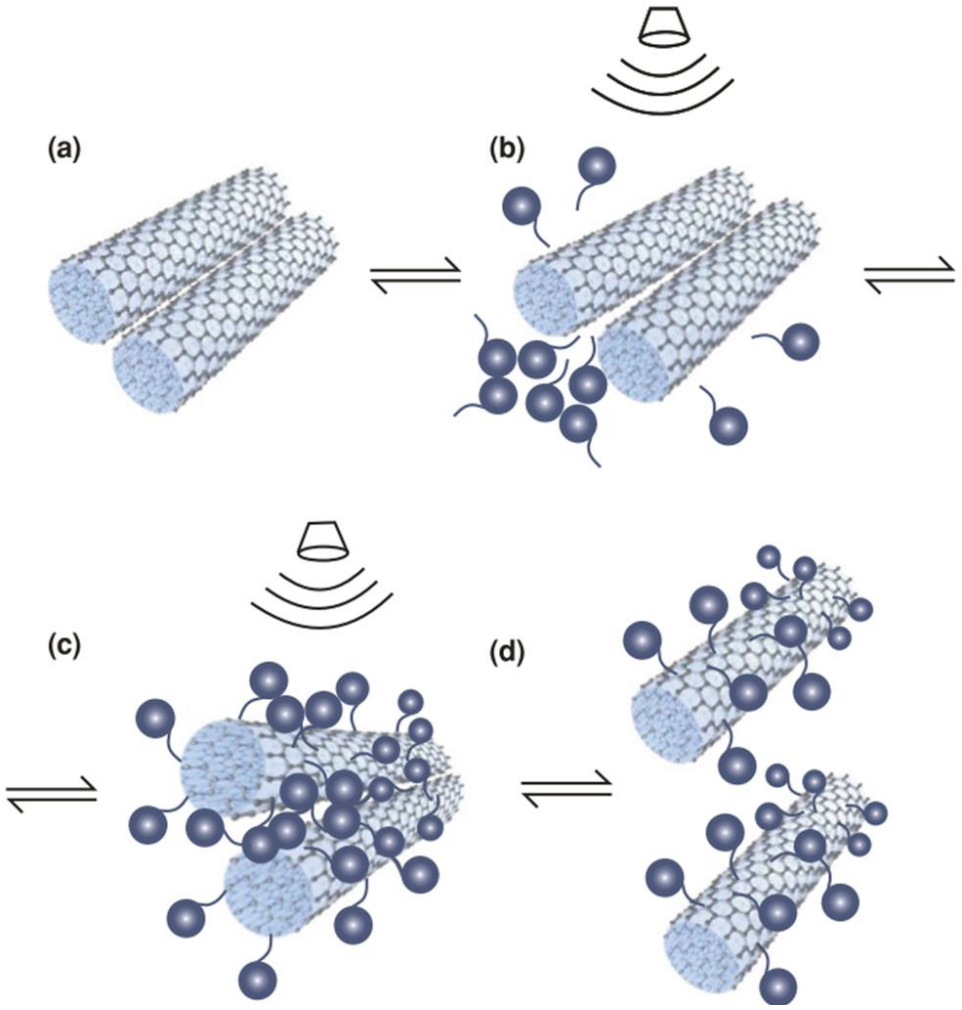

Figure 2.1 The process of dispersion of SWCNT by sonication with the aid of surfactants. Adopted from reference 29.

The surfactants used in this work include: sodium dodecyl sulfate (SDS), sodium cholate hydrate (SC) and sodium dodecyl benzenesulfonate (SDBS). The molecular structure of each surfactant is shown in (Figure 2.2). The efficacy of dispersing SWCNTs using different surfactants has already been described by Moore et al.,[51] in which they have tested various nonionic, anionic, and cationic surfactants to suspend HiPco nanotubes. They concluded based on observation of narrower, more distinct peaks in the optical absorption spectra that between different anionic surfactants tested, SDBS (Figure 2.2c) has the strongest effect of individualizing SWCNTs in an aqueous suspension.[51]

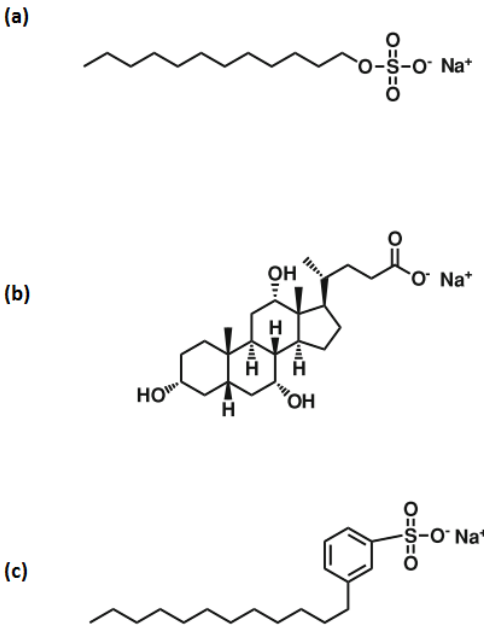

Figure 2.2 Molecular structure of the anionic surfactants used in this work: (a) SDS, (b) SC and (c) SDBS. Adopted from reference 29.

In order to prepare SWCNT suspensions, 2 mg of CoMoCAT SWCNTs (SG65i, Lot# SG65i-L39, SouthWest NanoTechnologies, Inc.) are added to 20 mL of 2 wt% surfactant solution. Ultrasonication is performed using a tip sonicator (Cole-Parmer, CP505). The power is set to allow the sonicator to run at 30% of its maximum amplitude (1/8" tapered microtip) yielding an output of ~12 W. The dispersion time is initially set to 60 minutes.[54] The samples are placed in a running water bath with temperature around 15 ^{o}C to avoid excess heat that can affect the ability of surfactant molecules to adsorb to the surface of SWCNTs.[55] The suspensions obtained after sonication are found to be dark in color with no observable aggregation (Figure 2.3).

Figure 2.3 SWCNT/SDS suspensions before sonication (left) and after (right).

The possibility of having catalyst particles in the SWCNT/surfactant suspension can affect the stability as well as the properties of the SWCNTs. Another issue that might arise is the presence of large clusters of undispersed nanotubes and amorphous carbon. These impurities are removed from the suspension by using centrifugation. In this step, a strong centrifugal force is applied to push larger particles to the bottom of a test tube. Bundles of SWCNTs are expected to have higher density than individualized SWCNTs. Consequently, they tend to travel to the bottom of the test tube leaving individualized SWCNTs at the top. Centrifugation is performed using a Hettich MIKRO 220 (1195-A 24-well angle rotor) with the conditions set to 18000 RPM, to obtain a radial centrifugal force (RCF) of 30790×*g*, and a total run time of 60 minutes to ensure removal of bundled undispersed SWCNTs. The top 75% of the volume of centrifuged tubes are collected in each step.

2.2 Separation of metallic and semiconducting SWCNTs

Separation of SWCNTs is driven by the desire to understand the distinct properties of both metallic and semiconducting species, and to fully exploit these properties in advanced applications. As described in Section 1.5, there are several

techniques that allow for the separation of metallic and semiconducting species of SWCNTs. Some techniques are preferred in some instances, such as electrophoresis, when aligned nanotubes are desired. However, full exploitation of the properties of SWCNTs can only be achieved via methods that allow industrial scale separation. Gel chromatography shows great potential since it combines the ability to obtain large scale separation output as well as being a cost effective process.

In this section, the process of separating CoMoCAT (SG-65i) SWCNTs is presented. The experiments described within are slightly modified from those described in the literature by Kataura et al.[37] More specifically, this work aims to reduce the total time and cost of the process making it more applicable to large industrial scale separation.

In this experiment, SWCNTs are dispersed in a solution containing 2 wt% SDS in deionized (DI) water. The mixture is sonicated for 60 minutes with an energy of ~12 watts following a centrifugation at 18000 RPM and 30790×*g*. Plastic 12 mL syringes are used as columns. Glass fiber is used to hold the stationary medium (described in more detail below) and keep it from leaking with the added surfactant eluent solutions or SWCNT/surfactant suspensions. Throughout this thesis, a Sephacryl gel (Sigma-Aldrich, S200HR, Lot# 120M1877V) is used as the stationary phase. A volume ratio of 1:1 SWCNT solution to gel is used as shown in Figure 2.4.

Figure 2.4 Image of loaded SWCNT/surfactant suspension on a gel medium.

Metallic SWCNTs tend to pass through the stationary medium showing minimum to no interaction with the gel. On the other hand, semiconducting SWCNTs tend to adsorb strongly to the gel medium and consequently are retained. This difference in affinity is described by the difference in packing density of SDS micelles around SWCNTs with different chiralities and electronic characters.[39,56] The effect of packing density was recently demonstrated by Hirano et al.[56] The original work presented a mechanistic insight into the separation by testing the effect of changing the pH of the SWCNT suspension and the subsequent ability for the SWCNTs to adsorb to the gel. The authors concluded that the higher packing density of SDS around metallic SWCNTs limits their ability to adsorb to the gel.[45,56] More recently, the process was described quantitatively by Tvrdy et al.[57] An SDS layer is related as providing a repulsive force between the Sephacryl binding sites and SDS/SWCNT structures. Thus, the higher density of SDS monomers surrounding the m-SWCNTs creates stronger repulsion, preventing them from adsorbing to the gel medium.

To release the retained SWCNTs in this experiment, a solution containing 1 wt% sodium cholate (SC) is used.[44] The elution of semiconducting SWCNTs is described as

the result of disturbance in the SDS micelles around SWCNTs adsorbed to the gel.[57] In this case, the adsorption of cholate groups onto the exposed regions of SWCNTs through hydrophobic-hydrophobic interaction results in reconfiguration of SDS molecules leading to the reduction in affinity of the supramolecular structure of SWCNT/SDS to the gel.[40] The obtained metallic and semiconducting SWCNT fractions are yellow and purple, respectively (Figure 2.5).

Figure 2.5 Separated metallic SWCNTs, "yellow fraction," and semiconducting SWCNTs, "purple fraction."

To compare the composition of the separated solution, optical absorption spectra are used to find the E_{11} and E_{22} transition peaks in the UV, visible, and NIR ranges. Each spectrum is measured from 240 to 1100 nm (Perkin-Elmer Lambda 25 UV-Vis) and normalized to 763 nm (Figure 2.6). The optical wavelength 763 nm allows for an easy comparison between samples with different electronic enrichment since most graphitic samples (SWCNTs as well as MWCNTs and graphenes) exhibit underlying absorption due to a C-C π-plasmon peaking in the UV and tailing off into this near infrared region, but there are no distinct SWCNT (n,m) species optical transitions to contend with. So, normalization accounts for the overall nanotube concentration differences while allowing

for the comparison of relative abundance of both metallic and semiconducting SWCNT species in different samples.

Metallic SWCNTs are expected to have allowed optical transitions (M_{11}) in the range between 350 – 490 nm. While semiconducting SWCNTs are expected to have E_{22} transitions between 475 – 820 nm and E_{11} transitions from 820 – 1200 nm.[27] The spectrum of the semiconducting fraction in Figure 2.6 shows a decrease in optical absorption in the region between 350 – 490 nm. This clearly indicates a successful enrichment of SWCNTs based on electronic type, in this case sc-SWCNTs.

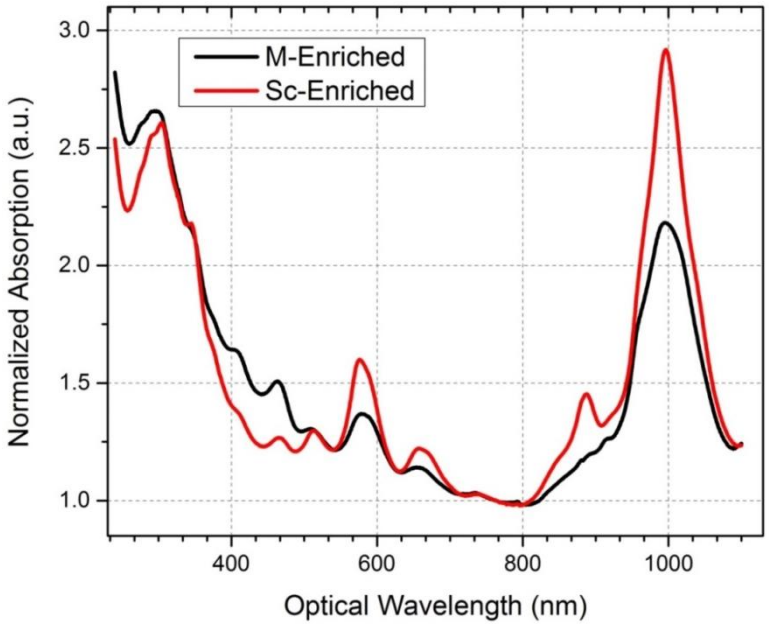

Figure 2.6 Absorption spectrum of metallic enriched (black) and semiconducting enriched (red). Spectrum is normalized to 763 nm.

The separated semiconducting SWCNT fraction is expected to have a number of (*n*,*m*) species, with (6,5) being the most abundant followed by (7,3), (8,1), (7,5), (9,1) and (6,4) (Appendix A1). The first van Hove (E_{11}) transitions of the dominant species of (6,5) and (7,3) are at 975 nm and 992 nm respectively.[58] However, the measured spectrum shows a single broad peak. This may be due to the inability of sodium cholate to fully individualize species within the narrow range of diameters.

In the metallic enriched fraction, the observed peaks between 970 – 1100 nm are due to the semiconducting nanotubes that pass through the medium without adsorption, possibly by being trapped in small bundles.[44,59] An increase in the optical absorption in the region of (M_{11}) between 350 – 490 nm (Figure 2.6) is a clear indication of a successful enrichment of metallic SWCNTs.

Previous work showed that even between semiconducting SWCNTs with different (*n,m*) indices, the process of adsorption becomes selective.[46,47] Assuming there's a finite number of adsorption sites on the stationary medium, one can selectively choose to retain a narrow range of (*n,m*) species with the smallest diameters simply by overloading a gel column.[46] In the previous experiment the volume ratio used was kept at 1:1 SWCNT solution / Sephacryl gel. Therefore one can argue that the volume of the gel is providing a sufficient number of binding sites to the majority of (*n,m*) species present in the sample.[46]

To test the effect of overloading a gel column on the eluted semiconducting enriched fraction, two columns are packed with the same amount of Sephacryl gel. The first column was loaded with a volume ratio of 1:1SWCNT suspension to Sephacryl gel, and the other is loaded 8:1. In the later, a large amount of SWCNTs pass through the medium and the first collected fraction is dark in color with no specific electronic enrichment. The high pass through supports the claim that only a finite number of adsorption sites are available in the stationary medium. In the column loaded with a volume fraction of unity, metallic enriched suspensions pass through the stationary phase and are collected. The retained sc-SWCNTs are then eluted using 1 wt% SC solution

from both columns. The composition of each fraction is determined through interpretation of the absorption spectrum (Figure 2.7).

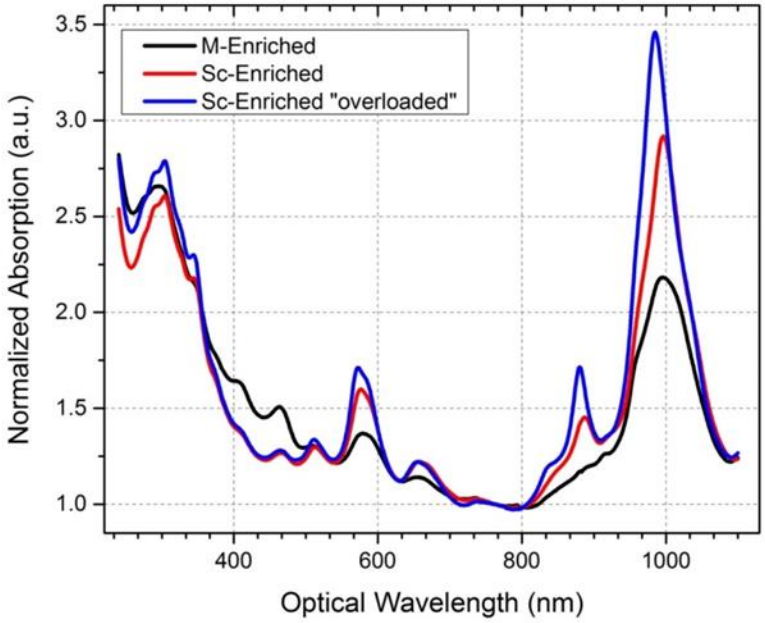

Figure 2.7 Absorption spectra of separated SWCNTs under different loading conditions. Spectrum is normalized to 763 nm.

The normalized spectrum in Figure 2.7 shows a noticeable increase in the E_{11} absorption region (960 – 1100 nm) which correspond to the (6,5), (7,5), (10,2), (8,3) and (7,3) species along with other peaks at ~833 and 875 nm which correspond to the (5,4) and (6,4).[60] The results show an overall enrichment of semiconducting SWCNTs in the sample where overloading conditions are used. The inability to eliminate a single chirality here is due to the presence of multiple (*n,m*) species with similar diameters, and thus column affinities, as described by the theory of Tvrdy et al.[46] However, the results obtained do not agree with what was reported by Kataura when HiPco SWCNTs were used.[44] This suggests that factors resulting from different production methods, such as average diameter, diameter dispersion, imperfections, and electronic enrichments, might

affect the thermodynamics of SWCNTs adsorption onto the gel. This motivates the need for further study in this area.

2.3 Separation of SWCNTs using alkali metal ionic salts

Since the publication of Kataura and co-workers,[47,59,61] which proposed a selective adsorption mechanism responsible for the retention of SWCNTs to the gel, many techniques have been developed based on this description such as multi-column chromatography[44] and temperature controlled single-chirality separation.[47] Despite the successful separation by electronic type, diameter, and chirality with gel filtration,[42,44,47,59,61] these methods have the disadvantage of high cost since they require the use of different concentrations of one surfactant or cosurfactants to release the retained SWCNTs in the gel medium.[51,52]

In this section, a simple and cost effective chromatography separation technique that employs aqueous solutions of alkali metal ionic salts to release the retained semiconducting SWCNTs from a stationary gel medium is demonstrated. The release of adsorbed tubes is described by the interaction between metal ions with the SWCNT/SDS complexes by changing the orientation of SDS molecules around the adsorbed SWCNTs.

Initially, when a pristine sample of SWCNTs is sonicated in the presence of a surfactant, SDS monomers tend to pack more densely around m-SWCNTs followed by larger diameter sc-SWCNTs (Figure 2.8).[39,62] Since larger diameter SWCNTs trend toward metallic character, this packing difference is potentially a result of differences in the electronic interactions between the SDS monomers and the metallic-like SWCNTs versus the small diameter sc-SWCNTs.. The illustrated difference in packing density of

SDS around SWCNTs in Figure 2.8 assumes a typical low concentration of surfactant (1 – 3 wt%) which is usually applied in physical adsorption experiments of SWCNTs.

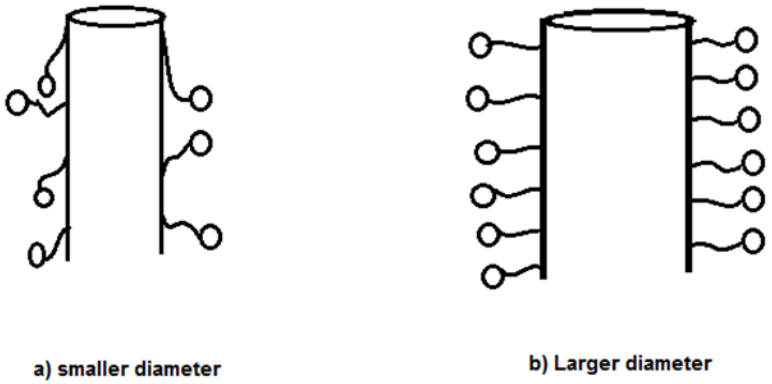

Figure 2.8 Packing density of SDS around SWCNTs. (a) Low packing density around smaller diameter SWCNTs, (b) high packing density around larger diameter SWCNTs.

When the concentration of surfactant is increased, the configuration is altered in both metallic and semiconducting SWCNTs and no difference in packing density is observed at high enough concentrations.[43] This explains the need to use low concentrations of SDS (< 2 wt%) in the initial suspension to ensure the adsorption of sc-SWCNTs which leads to successful separation.

2.3.1 The effect of salt on the adsorbed SWCNTs

The experiments in this section employ the same sample preparation steps described in the earlier section. Samples containing 2 mg of as produced CoMoCAT SWCNTs are dispersed in 20 mL of 2 wt% of SDS in DI water. Sonication time is set to 60 minutes with a power of ~12 W. Removal of large undispersed bundles is then achieved via centrifugation for 60 minutes and centrifugal force of 30790×*g*. Plastic 12 mL syringe columns with glass fiber are packed with 4 mL of Sephacryl-S200. Initial washing of the column is done using a solution of 0.5 wt% SDS in DI water. Loading conditions are maintained at a volume ratio of 1:1 of Sephacryl to SWCNT/SDS suspension.

In each column, metallic enriched SWCNT suspensions are collected as they pass through the stationary medium showing minimum interaction. On the other hand, semiconducting SWCNTs/SDS tend to interact strongly and adsorb to the gel. The difference in the affinity is attributed to the packing density of SDS micelles around SWCNTs with different geometry configurations.

At the conventionally used concentrations of SDS (1 – 3 wt%) it is energetically favorable for the hydrophobic tails to assemble in a flat and less dense manner along the surface of smaller diameter SWCNTs which keeps the surfactant head groups closer to the surface.[43] On the other hand, charged head groups remain at a distance away from the surface in metallic SWCNTS. This difference in configuration is used to describe the difference in affinity of SWCNTs towards the gel. If the interaction is assumed to be mainly due to the configuration of SDS micelles around the SWCNTs, then it is possible to elute the retained semiconducting SWCNTs in the gel medium just by inducing changes in the SWCNT/surfactant micellar structure.

In the conventional SWCNT chromatography reported in the literature, two different methods are used to elute the semiconducting fraction from the gel. One method uses a cosurfactant as described in section 2.2. Another technique employs a higher concentration of the same surfactant (e.g. 5 wt% of SDS)[59] to obtain the retained SWCNTs from the gel. Both approaches are described by the adsorption of surfactant micelles in the eluting solution onto the exposed regions of the nanotube. Thereby increasing the number of SDS monomers per unit area (aggregation number) and altering the configuration around the retained SWCNTs.[40] This leads to an increase in the repulsive forces with the gel which reduces the affinity of the supramolecular to the gel.[57]

In contrast, a new approach for elution of the SWCNTs adsorbed to a Sephacryl gel is taken in this work. The retained SWCNTs are released from the gel by introducing aqueous solutions containing alkali metal ionic salts. The effect of salts on pure SDS micelles (i.e. no nanotubes present) has been the subject of study for a long time in colloidal chemistry.[63] Previous experiments on pure SDS in water reported a decrease in the critical micelle concentration (CMC) as the concentration of salt is increased in the solution, as well as, an increase in aggregation number.[63,64] This indicates that salts can be used to induce changes in the SDS configuration around SWCNTs which in turn will affect the overall affinity of the SWCNT/SDS to the gel.

To test the effect of salts on the separation of SWCNTs, first, a solution containing 295 mM NaCl in DI water is used to elute adsorbed SWCNTs from Sephacryl gel. The introduction of a salt solution serves as a charge screening medium by which the electrostatic interaction of cations with the negatively charged sulfate group on the SDS micelle results in the transformation of the configuration of SDS from being randomly oriented to rod like structures perpendicular to the surface of the SWCNT.[60] Consequently, the affinity of SWCNT/SDS micelles with the gel medium is reduced and the retained nanotubes are eluted. The collected semiconducting fractions are purple in color as expected from a (6,5) enriched sample (Figure 2.9).

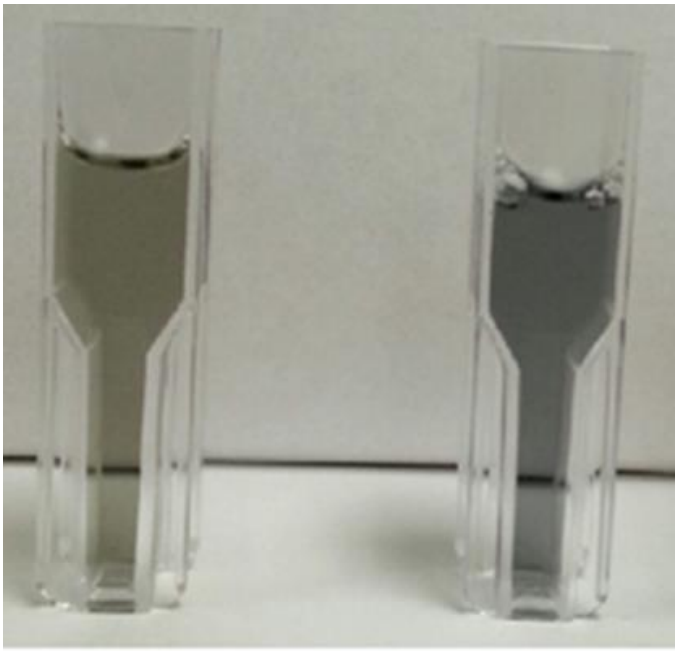

Figure 2.9 Separated yellow "metallic," and purple "semiconducting" SWCNT fractions after addition of 295 mM NaCl.

Although the purple color of the eluted sample is a clear indication of a successful separation, the abundance of each individual (*n*,*m*) SWCNT type can be determined by absorption spectroscopy. Absorption spectra are measured over the visible to near-infrared range of 400 to 1100 nm (Figure 2.10).

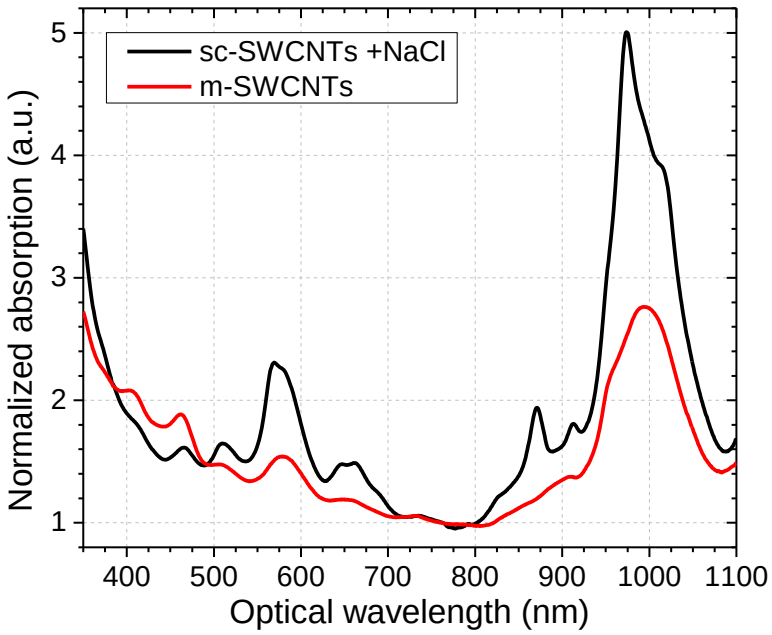

Figure 2.10 Absorption spectra of a sample separated with 295 mM NaCl to yield sc-SWCNTs (black). The separated m-SWCNT fraction (red) collected initially is shown for comparison.

The normalized spectrum shows the distinct peaks for the E_{11} transitions of the (6,4) at 873 nm, (6,5) at 975 nm, (7,3) at 992 nm, and (7,5) at 1024 nm.[60] The second van Hove (E_{22}) transitions are also observed for the same species with (7,3) at 507 nm, (6,5) at 567 nm, (6,4) at 578 nm, and (7,5) at 645 nm.[65] On the other hand, the m-SWCNT enriched sample displays enhanced absorbance in the M_{11} region (Figure 2.10).

To understand how the method developed here differs from the conventional two surfactant technique, two side by side columns are tested. One is separated by a solution of [NaCl] (<1 wt%) and the other is separated with 1 wt% sodium cholate as a cosurfactant (Figure 2.11).

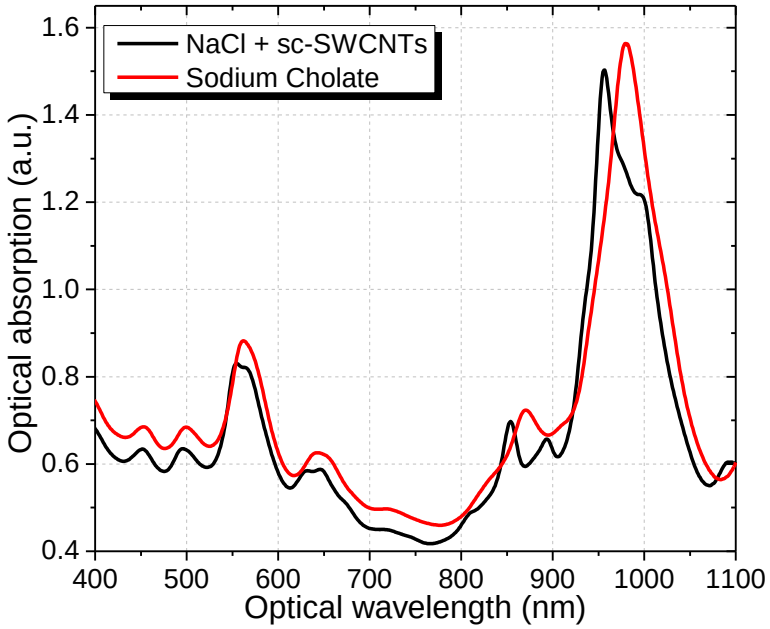

Figure 2.11 Absorption spectrum of semiconducting SWCNTs separated with NaCl (black) and SC (red).

The absorption spectra (Figure 2.11) show more noticeable distinct peaks in the sample separated with NaCl. This implies that samples containing salt display higher degree of electrostatic repulsion between different SWCNT/SDS complexes in the narrow diameter range giving more individualized nanotubes in the collected fractions. Moreover, these non-normalized spectra indicate the total SWCNT yield is similar whether a salt solution or a cosurfactant is used. This can be deduced by comparing the height of most dominant species (6,5) in both solutions, or using the absorbance value at 763 nm described earlier.

2.3.2 Anions and cations in the eluting solution

If the modification of SDS structure is mainly due to charge screening from charged ions, then using salts with different metal cations or different anions to elute the sc-SWCNTs from the gel should lead to similar results obtained with NaCl but possible trends related to ionic size would be revealed. To test this hypothesis, a series of

separation experiments are performed using the same molar concentrations of metal salts, but with NaI and NaSCN to understand the effect of using a salt with larger anion. Absorption spectra of separated samples are taken immediately after separation (Figure 2.12).

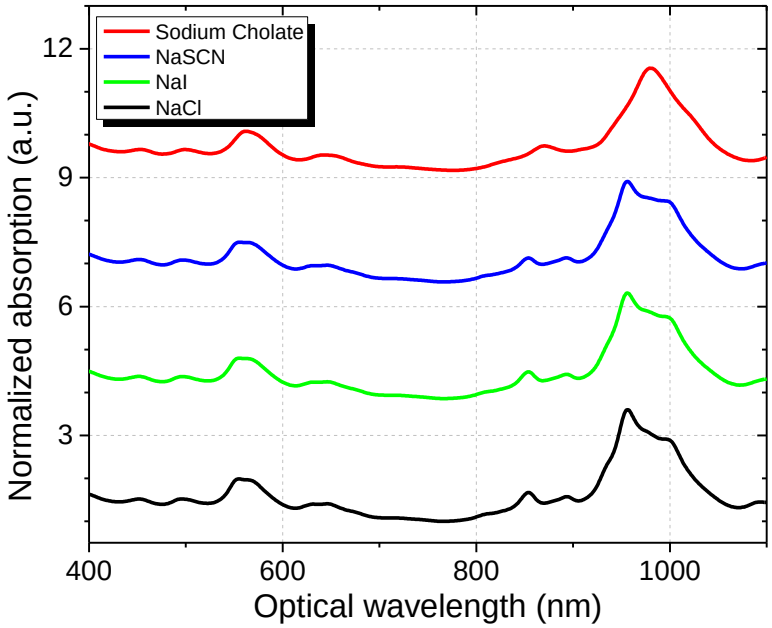

Figure 2.12 Absorption spectrum of semiconducting SWCNTs separated with NaCl (black), NaI (green), NaSCN (blue) and 1% sodium cholate (red). Profiles are normalized to 763 nm.

The profiles in Figure 2.12 do not display any differences between the samples eluted with salts having different anions. This suggests that the main driving factor in the separation is the concentration of positively charged metal cations. Although the effect of anion structure and size is not clear, the samples containing larger anions displayed lower stability and displayed aggregation after a short period (< 3 days). One can suggest that in the samples separated with larger anions, the charge of the supramolecular structure is neutralized. In other words, the micelles are no longer adsorbed to the nanotubes. In contrast, the samples separated with NaCl displayed observable stability over a long period (~10 days). It is important to note that the sample separated with sodium cholate

contained a different molar concentration of metal ions versus NaCl. At 1 wt% of SC, the concentration of Na ions is much lower than 295 mM. Therefore, the elution with sodium cholate cannot be considered a result of reconfiguration of micelles due to Na^+ but more likely the adsorption of the cholate ions on the exposed regions of SWCNTs via π- π interactions.

The effect of cations on the separation is tested by using different salts such as LiCl and KCl. The same procedure is followed to test salts with different cationic groups. The collected fractions at the same molar concentration of salt are shown in (Figure 2.13)

Figure 2.13 Separated metallic "yellow" and semiconducting fractions with different salts. LiCl (transparent), NaCl (purple) and KCl (grey aggregates).

Samples separated with KCl showed immediate aggregation with gray color, while the samples eluted with LiCl were optically transparent (Figure 2.13). The difference in color between the fractions collected with different alkali metal salts suggests a relation between the size of the ion and the ability to elute SWCNTs from the medium. If the solution eluted with KCl is displaying aggregation, it is reasonable to assume that the concentration of metal ions required to elute SWCNTs from the gel depends on the size of the metal ion. Following this assumption, the concentration of KCl is reduced to 67 mM and the concentration of LiCl is increased to 1.179 M in the eluting

solution. The absorption profiles in Figure 2.14 show the spectra of the successfully eluted semiconducting SWCNT fractions.

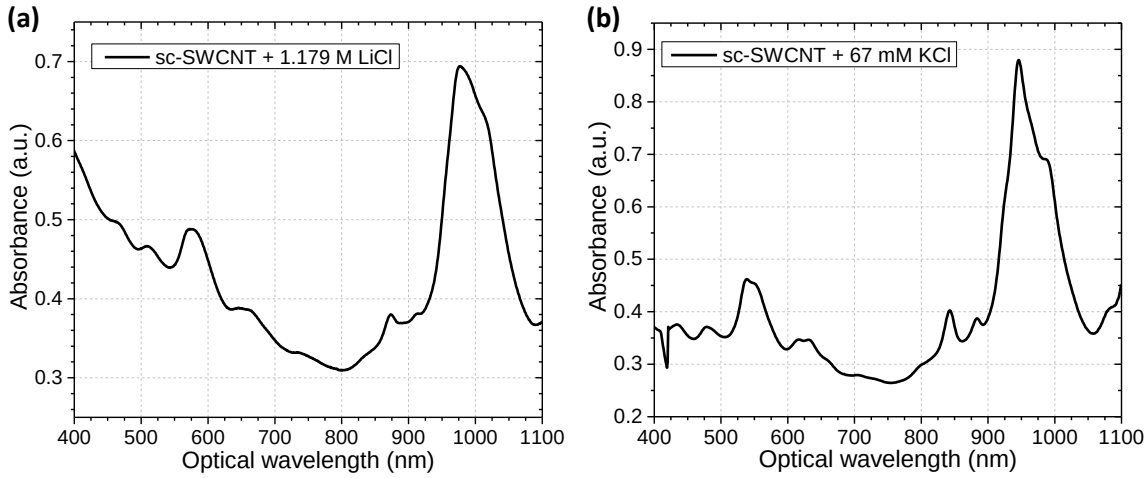

Figure 2.14 Absorption spectra for sc-SWCNTs collected following the addition of (a) 1.179 M LiCl, (b) 67 mM KCl.

The variation in interaction of different metal ions with the SWCNT/SDS micelles is similar to previous explanations in the literature describing a change in hydration for different metal ions. That is, the smaller Li ion is surrounded by more water molecules making it more difficult for the ion to get closer to and interact with the SDS sulfate headgroup.[66]

2.3.3 Concentration of NaCl and (*n*,*m*) composition

To test the effect of varying the ionic strength on the amount of SWCNTs eluted from the gel as well as the possibility of selective (*n*,*m*) enrichment in the semiconducting fractions, the concentration of NaCl in the eluting solution is varied between 45 to 513 mM. Following the same steps described in the previous section, four identical columns were run, each one loaded with a volume ratio of 1:1 SWCNT/SDS suspension to Sephacryl. The collected sc-SWCNT fraction from each column is characterized using absorption spectroscopy (Figure 2.15).

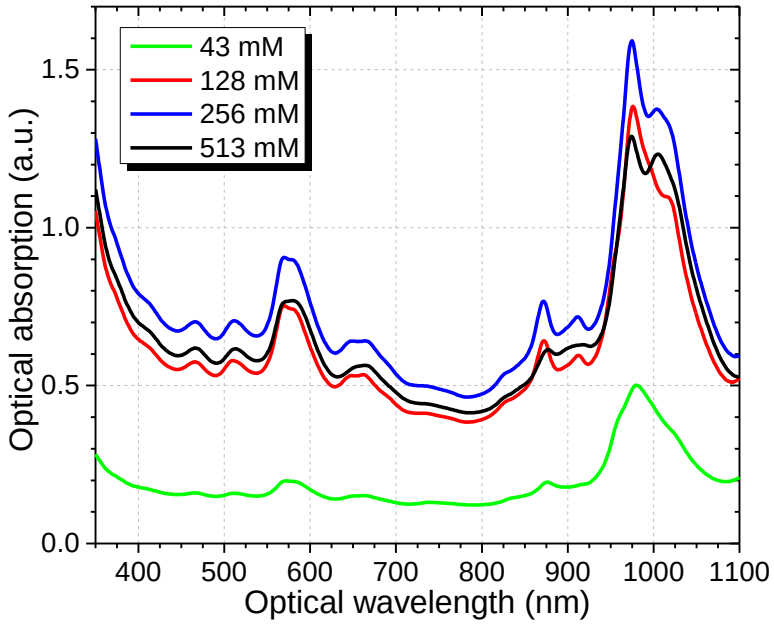

Figure 2.15 Absorption spectra of sc-SWCNT samples separated with different concentrations of NaCl.

The samples collected at low concentration of 43 mM are dilute and display a light blue color. This indicates that only a small fraction of adsorbed SWCNTs are eluted. The relative height of observed (*n*,*m*) peaks are considerably lower than the samples containing higher concentrations of NaCl. Interestingly, when the concentration is increased to 513 mM the peak heights of the dominant species, (6,5) and (7,3), were decreased (Figure 2.15). The obtained results provide a hint that a relationship between the concentration of NaCl and the (*n*,*m*) composition of the eluted fractions might exist. For instance, at high salt concentrations aggregation occurs (Fig 2.13 and 2.14b), so the observations here may be indicating the onset of (*n*,*m*) or diameter specific aggregation. This relationship is considered further in the next section.

2.3.4 Fitting analysis of optical spectra

The full understanding of the separation process and the investigation of composition of samples eluted with NaCl is achieved with peak fitting of the experimentally observed spectra.

There are many problems that arise when trying to mathematically model the absorption spectra of SWCNTs solutions. One is the existence of many (*n,m*) species with bandgap energies not well separated. Another problem is the difference in surfactant packing around SWCNTs with different diameters. This results in having different degrees of exposure of the SWCNTs in the suspension. Smaller diameter species are thus expected to be more exposed to the surrounding aqueous environment than larger diameter species.[39,62] Therefore, it is reasonable not to fix the peak widths when trying to simulate the individual (*n,m*) peaks.

Previous work by several groups, including Weisman at Rice and Strano at MIT, tested different mathematical functions in an attempt to reach the best fit for absorption spectra.[67] Between three different spectroscopic functions: Gaussian, Lorentzian and Voigt, the best fit was obtained by using the Voigt function (equation 2.1).

$$V = V_{\circ} + A \cdot \frac{2\ln(2)}{\pi^{3/2}} \frac{w_L}{w_G^2} \cdot \int_{-\infty}^{\infty} \frac{e^{-t^2}}{\left(\sqrt{\ln(2)}\frac{w_L}{w_G}\right)^2 + \left(\sqrt{4\ln(2)}\frac{x - x_C}{w_G} - t\right)^2} dt \qquad (2.1)$$

Equation 2.1 is a convolution of a Gaussian and Lorentzian profiles where V_o represents the offset, A is the area, W_G and W_L represent the Gaussian and Lorentzian widths respectively, x_c is the center location of the peak and t is the horizontal axis, in this case wavenumber.

The goal of spectral analysis here is to compare the relative composition of sc-SWCNT samples eluted with different fractions of NaCl. This is achieved by focusing on the E_{11} region of the spectrum (830 – 1100 nm) where the transitions of the most abundant species are present.

Unlike the model developed by Strano et al. where it only accounted for background plasmon absorption and individual (*n*,*m*) peaks,[67] here, the proposed model also accounts for noise signals generated by the instrument. In this case, the total absorption can therefore be represented by

$$A_{total} = A_{(n,m)} + A_{Background} + A_{noise} \qquad (2.2)$$

Where $A_{(n,m)}$ is absorption of (*n*,*m*) SWCNTs, $A_{background}$ is the absorption due to colloidal graphite and its surface plasmon, and A_{noise} is the noise signal generated by the instrument. After converting the obtained experimental dataset to an energy scale (cm^{-1}), a linear absorption background is constructed by connecting the minimum absorption points via a straight line (Figure 2.16).

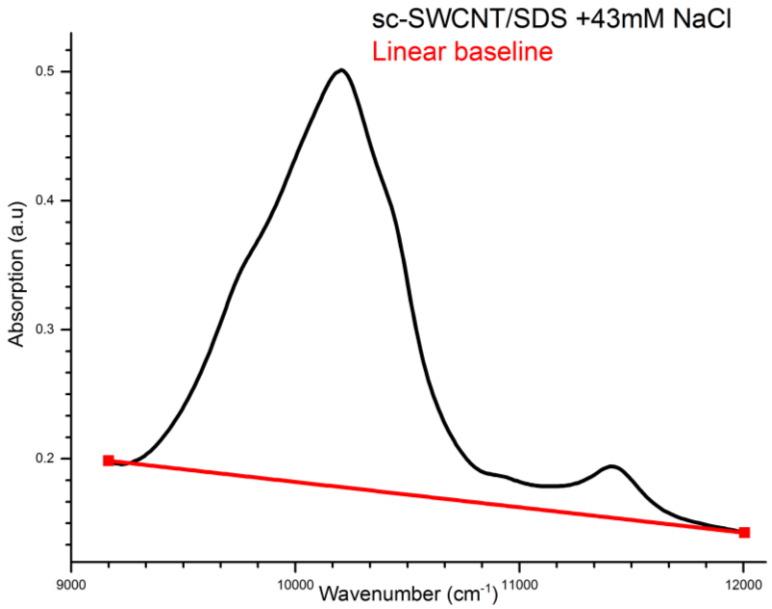

Figure 2.16 Illustration of linear baseline subtraction in the chosen region.

The effect of noise is eliminated by applying a Fourier transform filter to the second derivative of the measured signal to reduce the possibility of having peaks which (*n*,*m*) values cannot be assigned to. This also helps identify the initial center locations of 8 different (*n*,*m*) SWCNT species at the same time (Figure 2.17).

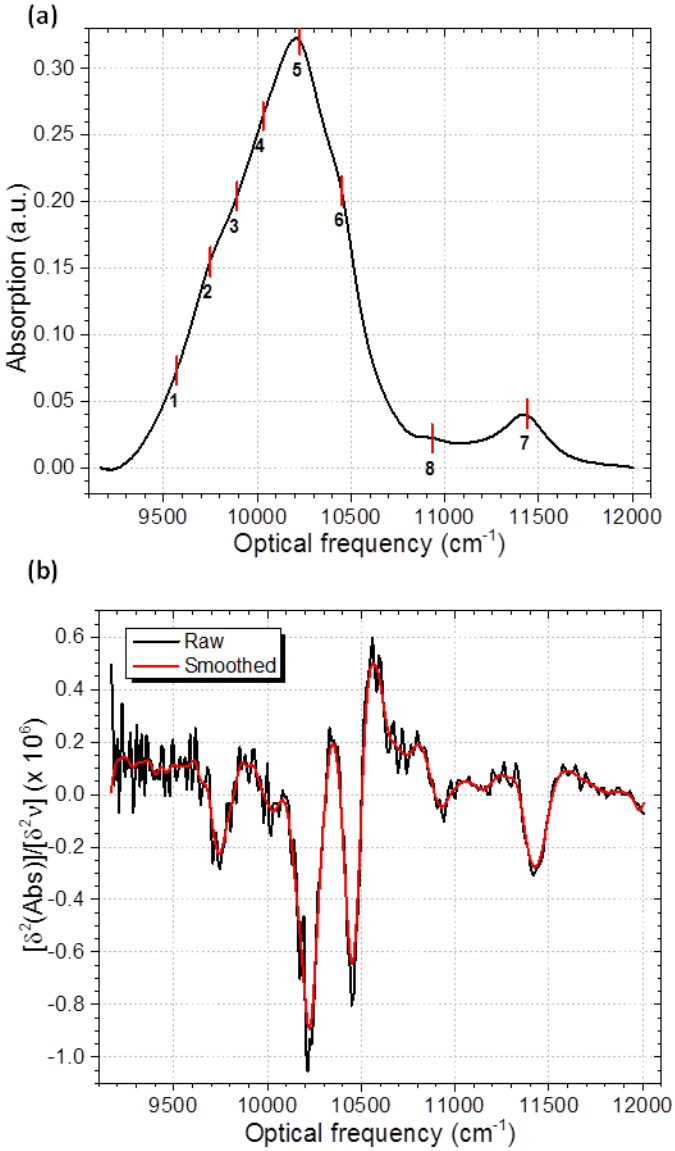

Figure 2.17 Absorption spectrum of sample separated with 43 mM NaCl (a) location of different (*n*,*m*) peaks, and (b) second derivative of the spectrum.

Once the noise is eliminated the total absorption can be assumed to be the sum of individual Voigt functions representing each (*n*,*m*) species. Assuming equal extinction coefficients of different SWCNTs, the spectrum of the selected region is represented as

$$A_{sim} = \sum_{1}^{k} C_{(n,m)} V_{(n,m)} \tag{2.3}$$

Where k is the total number of basis functions, $V_{(n,m)}$ represents the Voigt function used to curve fit the first van Hove transition of SWCNTs with (n,m) indices, and $C_{(n,m)}$ is the respective (n,m)-species relative concentration.

An iterative process, using the curve fitting routines in OriginPro 9.1, on the spectra obtained with different concentrations of salt is performed. Before fitting each spectrum one has to set photophysical boundaries that would give reasonable results. This is done by fixing the baseline to zero to eliminate negative peaks and varying the peak widths of SWCNTs within a range of less than 500 cm^{-1} to obtain the best fit. The fitting process here depends on minimizing a statistical variable, χ^2,which is mathematically defined as

$$\chi^2 = \sum_{i=1}^{n} \left[\frac{A_{obs} - A_{sim}}{\sigma_i} \right]^2 \qquad (2.4)$$

where σ_i is the local variance and A_{obs} and A_{sim} are the observed and simulated absorption signals, respectively. The value of χ^2 approaches zero when the fitted signal agrees with the experimentally measured signal.

The assignment of (n,m) values is done by tracking the change in the smoothed curvature of the spectrum (Figure 2.17b). The location of each peak is then compared with previously obtained experimental values.[65] The simulated absorption spectrum of the sample containing 43 mM of NaCl is shown in Figure 2.18.

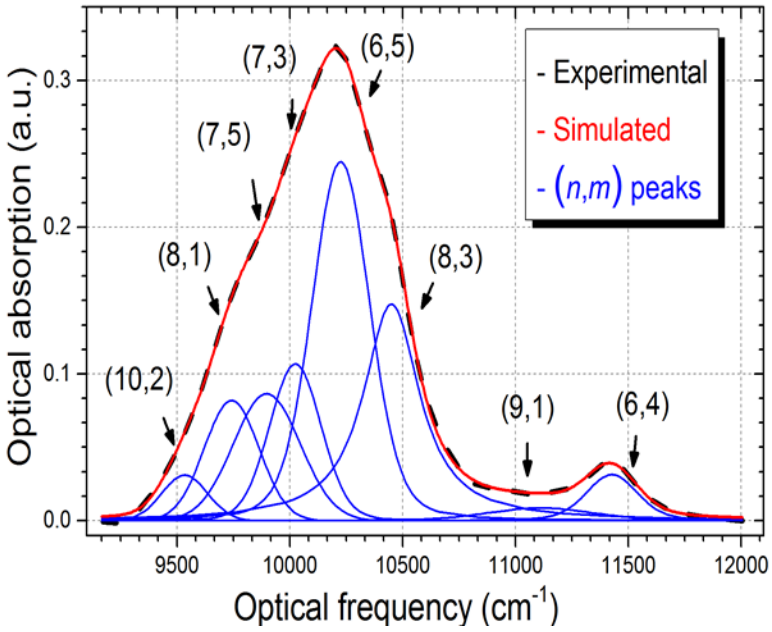

Figure 2.18 Fitted absorption spectrum showing simulated signal (red), measured signal (black), and individual (*n*,*m*) peaks (blue).

The individual peaks had different linewidths. This is explained by the difference in surfactant wrapping around SWCNTs having different diameters. The values of full width half max (FWHM) are in the range between 200 – 350 cm^{-1}. For comparison, the values obtained for FWHM are greater than those proposed by Strano et al.[67] where it was assumed to be fixed to 200 cm^{-1} for all SWCNT species. The relative concentration of each species, $C_{rel,(n,m)}$, is then deduced using the relation

$$C_{rel,(n,m)} = \frac{\int A_{(n,m)}}{\int A_{sim}} \times 100 \qquad (2.5)$$

The denominator in equation 2.5 represents the area integral of all the simulated peaks. The values of $C_{rel,(n,m)}$ are calculated from a series of simulations for each experimentally observed spectrum. For different experiments, the relative concentrations vary slightly. Therefore, an average of four simulation experiments starting with slightly different guesses were conducted to determine the average $C_{rel,(n,m)}$ and a standard

deviation (% error) for the obtained values, as tabulated in Table 2.1. The relative concentrations are plotted on a graphene sheet map (Figure 2.19) to visually compare the detected (*n*,*m*) species with different diameters and chiral angles.

Table 2.1 Relative abundance of (*n*,*m*) SWCNTs at different concentration of NaCl.

	[NaCl] 43 mM		**[NaCl] 128 mM**		**[NaCl] 256 mM**		**[NaCl] 513 mM**	
(*n*,*m*)	**Average $C_{rel,(n,m)}$ (%)**	**σ**	**Average $C_{rel,(n,m)}$ (%)**	**Σ**	**Average $C_{rel,(n,m)}$ (%)**	**σ**	**Average $C_{rel,(n,m)}$ (%)**	**σ**
(10,2)	2.94	0.18	3.15	0.59	0.60	0.74	0.10	0.22
(8,1)	9.46	0.16	5.57	0.89	8.88	1.50	10.95	1.80
(7,5)	12.17	0.34	12.24	0.44	8.13	0.36	3.68	1.50
(7,3)	13.22	1.86	25.61	1.28	27.72	1.15	34.61	1.64
(6,5)	32.59	0.18	32.67	1.06	37.05	0.80	31.51	2.20
(8,3)	23.09	2.24	7.29	0.20	5.65	0.61	8.02	2.31
(9,1)	2.74	1.02	7.41	0.28	5.46	0.82	5.14	0.30
(6,4)	3.75	0.13	6.02	0.49	6.47	0.33	5.95	0.27

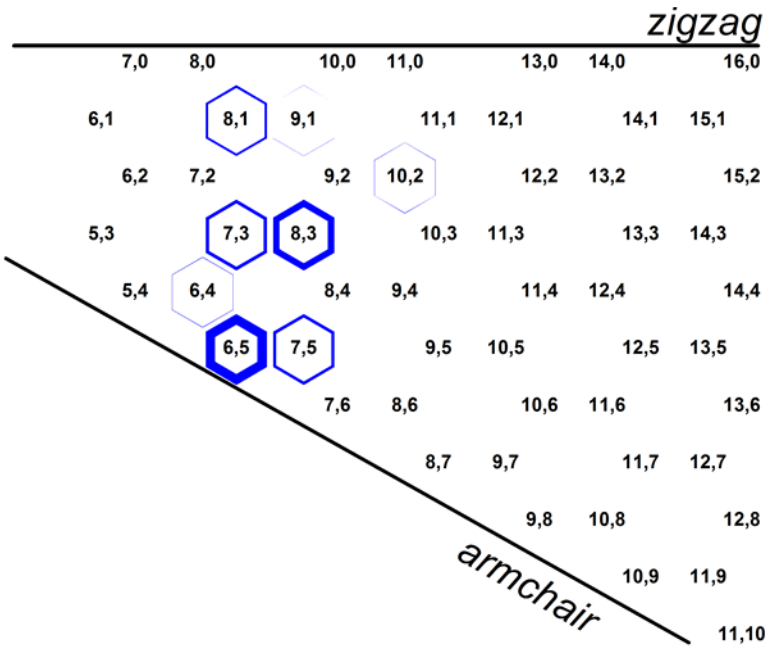

Figure 2.19 Relative concentration of detected (*n*,*m*) species with (6,5) being most abundant.

The same statistical fitting procedure is followed with the samples containing different concentrations of NaCl. The results are plotted in Figure 2.20. By observation, an increase in profile width of larger diameter species such as (10,2) and (7,5) when the concentration of salt is increased in the eluting solution suggests that some form of aggregation is taking place. This is followed by a decrease in the relative abundance of the mentioned species. This can also be traced by observing the change in the average concentration of the these species at different ionic strengths in Table 2.1.

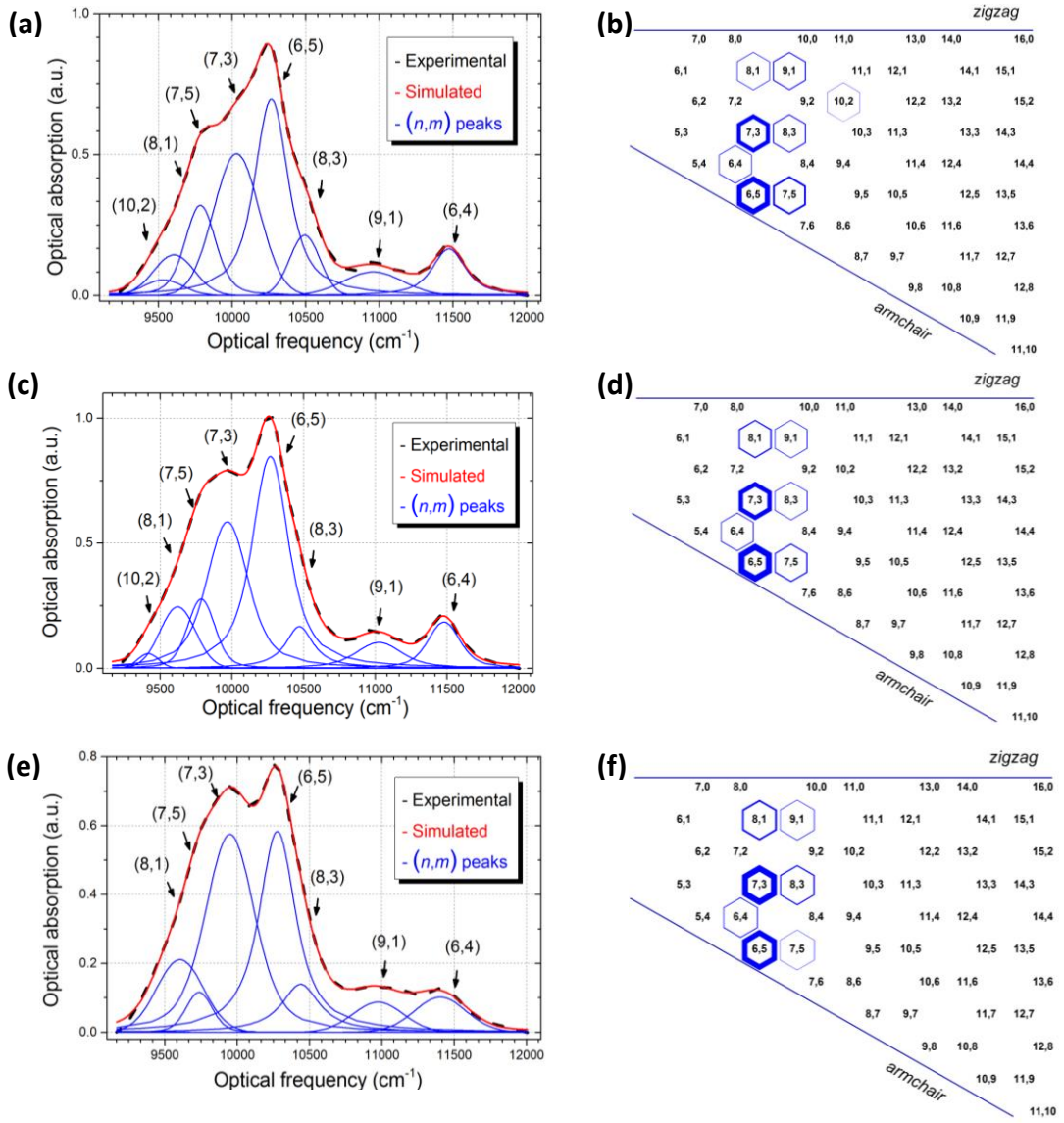

Figure 2.20 (a,c,e) Fitted absorption profiles at different concentrations of NaCl, (b,d,f) Relative sc-SWCNT (*n*,*m*) species based on absorption simulations.

2.4 Conclusions

This work demonstrates the ability to separate single-walled carbon nanotubes by their electronic character using different alkali metal ionic salt solutions during gel chromatography. The structural arrangement of SDS micelles around SWCNT molecules is altered by the addition of salt ions leading to the improved elution of both m- and sc-SWCNTs from the gel medium. Different alkali metal salts including KCl, LiCl, NaCl,

NaI and NaSCN were used in the separation process, and while the separation process is found to be driven by the concentration of cations in the eluting solution, the stability of separated samples is affected by the size of the anion. solutions separated with larger anions displayed less stability. Between the different salts, NaCl is demonstrated to give the best results in terms of individualizing the nanotubes as observed from the absorption spectrum. One can hypothesize that this is a consequence of the CMC of SDS around SWCNTs and the ability of Na^+ to gradually increase the aggregation number of SDS without causing complete aggregation. Modeling the experimentally observed absorption profiles demonstrates that aggregation starts in larger diameter SWCNTs when the concentration of NaCl is increased in the eluting solution. The results imply that it is possible to fine tune the concentration of NaCl in the eluting solution in order to selectively enrich a solution with specific (*n*,*m*) species.

CHAPTER 3: THIN-FILMS OF SEPARATED SINGLE-WALLED CARBON NANOTUBES

3.1 Deposition of SWCNT films from organic solvents.

The deposition of SWCNTs on substrates like glass is of major interest for many applications including biological imaging, optoelectronic fabrication and nanoelectronic devices.[68,69] Significant research emphasis currently is geared toward determining a deposition method which can yield large area films of uniform and aligned SWCNTs. Several deposition techniques reported in the literature include vacuum filtration,[70] dip coating,[71] spin coating[72] and evaporation driven self-assembly.[73]

The main focus in this section is on extracting SWCNTs from their surfactant solution and dispersing them in organic solvents for deposition. The sorting methods described in the previous chapter yield electronically separated SWCNTs suspended in surfactant. The problems that arise when trying to spin coat separated SWCNTs are the presence of surfactant which limits their ability to deposit on glass. Another problem is the difficulty of deposition from an aqueous solution.[74] Therefore, an alternative approach to solve the problem is to spin coat SWCNTs from an organic solution free of any surfactants. However, this still means that separated SWCNTs must be stripped from the surfactant micelles.

Previous work by Meitl et al.[75] demonstrated the ability to remove the surfactant from SWCNTs right before they are coated on a substrate. This is achieved by creating a diffusion layer formed by simultaneously introducing methanol and the SWCNT/SDS aqueous suspension onto the spinning substrate (Figure 3.1).[75,76] The SDS micelles are removed by having higher affinity toward the organic surrounding. However, precise control of deposition conditions remains a challenge. Therefore, a slightly modified

approach is followed in this section to achieve highly enriched single electronic character SWCNTs in methanol or acetone.

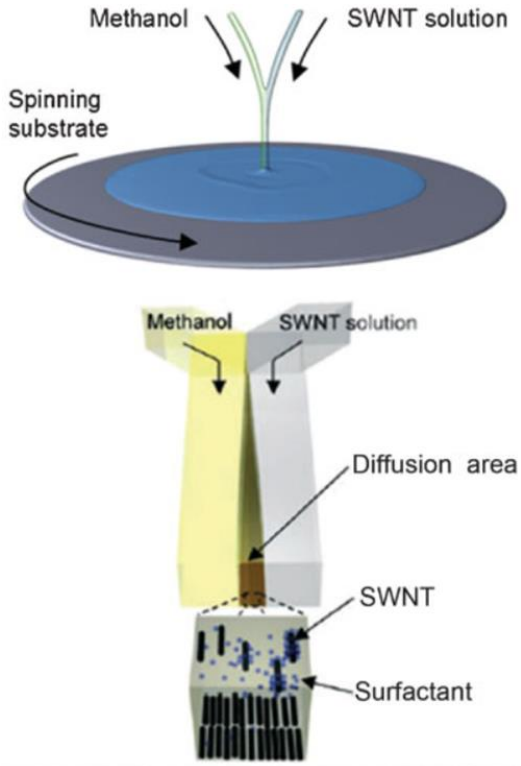

Figure 3.1 Illustration of a proposedprocess for surfactant removal and SWCNT spin coating. Adopted and modified from reference [76].

Following the assumption of Meitl et al. that SDS monomers have higher affinity towards the organic solvent,[75] the addition of a sufficient volume ratio (3:1) of methanol or acetone to SWCNT/SDS suspensions is found to cause observable aggregation as shown in Figure 3.2a. The exposure of the SWCNT surfaces, as a result of SDS removal, causes them to interact with each other via van der Waals forces. When the mixture of SWCNT/SDS and organic solvent is subjected to a centrifugal force (1500 RPM, <1000×*g*) for a short period of 4 minutes (Figure 3.2b), SWCNTs are forced to sink forming aggregates at the bottom of the tube (Figure 3.2c). The success of the process is governed by the amount of organic solvent used to extract SDS molecules from the SWCNT surface.

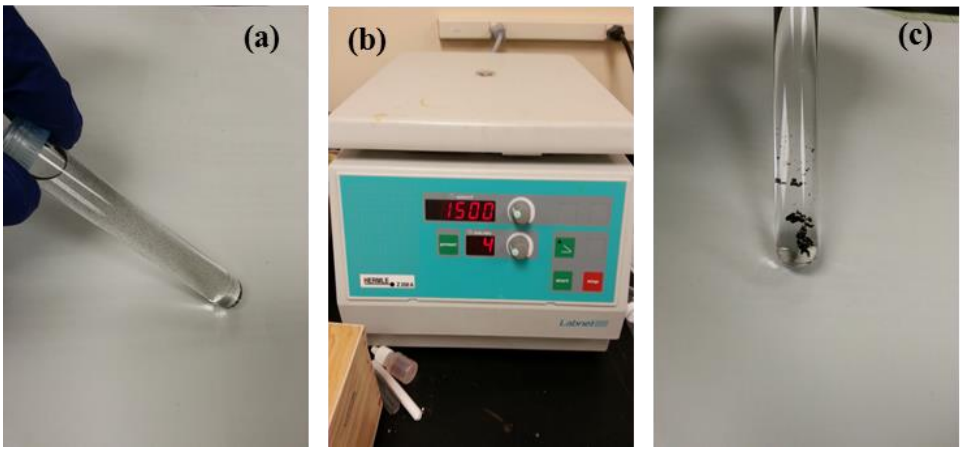

Figure 3.2 The process of surfactant removal from SWCNTs: (a) addition of methanol or acetone to SWCNT/SDS solution, (b) centrifugation of mixture, and (c) aggregated SWCNTs free of surfactant.

In the case when the concentration of SWCNTs is high, a repetitive process of organic solvent addition, centrifuging, and removing the top portion is required. The bundled SWCNTs are then redispersed in an organic solvent (e.g. methanol, acetone, or dimethyl formamide) through sonication for 30 minutes at a power of ~12 W to produce a suspension that is stable for 3 – 10 mins depending on the concentration of SWCNTs. These suspensions can then be spin coated onto glass substrates at the desired conditions.[72]

SWCNTs deposited on different substrates following the described method can be characterized using different microscopy techniques such as atomic force microscopy (AFM) or scanning electron microscopy.[77]

3.2 Vertical deposition from aqueous solutions.

Between different methods for depositing SWCNTs from a surfactant suspension, vertical deposition offers a simple and cost effective method for deposition.[78] In this method, a substrate is inserted vertically into an aqueous suspension of surfactant wrapped SWCNTs. The water is then evaporated at a certain rate causing the

SWCNT/surfactant to form a highly ordered crystalline structure on the substrate. Several variables are controlled in this process such as the concentration of surfactant and SWCNTs, evaporation rate, and the angle of contact.

The quality of the produced films is assessed with various methods that look at the order of the crystal. Such methods may include scanning electron microscopy (SEM) and atomic force microscopy (AFM), which can be used to address the domains of ordered structures, as well as, the thickness of the produced films.

In the case of semiconducting SWCNT films, the existence of unique (*n,m*) optical transitions allows the use of more simple and cost effective methods such as absorption and fluorescence to investigate the possibility of van der Waals interaction between different SWCNTs. This is achieved by looking at the optical absorption profile where the presence of distinguishable (*n,m*) peaks is an indication of minimized interaction between SWCNTs. The present work will use absorption spectroscopy as well as optical microscopy to characterize SWCNT films produced with this method.

The suspended SWCNT/SDS structures experience Coulombic forces resulting from the interaction of surfactant charged heads with each other and metal ions in the solution. Another force experienced by SWCNTs in the solution is the gravitational force. Even in solutions of separated SWCNTs there is a mixture of different (*n,m*) species having different buoyancies due to factors such as surfactant wrapping and SWCNT geometry.[79,80] Also, suspended SWCNTs experience diffusional motion in their environment, which is dependent on the (*n,m*) species, the surfactant and its micellar structure with the SWCNT, and the solvent viscosity.[81,82] Some of these factors increase

diffusional rates, like small diameter SWCNTs, while others, such as solution viscosity, decrease the diffusion.

When the solution is subjected to a heat source, water starts to escape from the medium leaving SWCNT/surfactant to diffuse. If the diffusion velocity of, in these studies, the SWCNT/SDS complex is lower than the velocity of the interface which is dropping due to evaporation, the concentration of SWCNT/SDS complexes near the water/air interface increases. Along with diffusion and viscous forces responsible for controlling the SWCNT/SDS concentration profile, the Coulombic repulsion between SDS sulfate headgroups forces the concentrated SWCNT/SDS complexes to align into an ordered structure.[78] Therefore, the presence of a charged (anionic, in this case) surfactant is an essential part that drives the alignment of SWCNTs near the water/air interface. A graphical description of the assembly is shown in Figure 3.3.

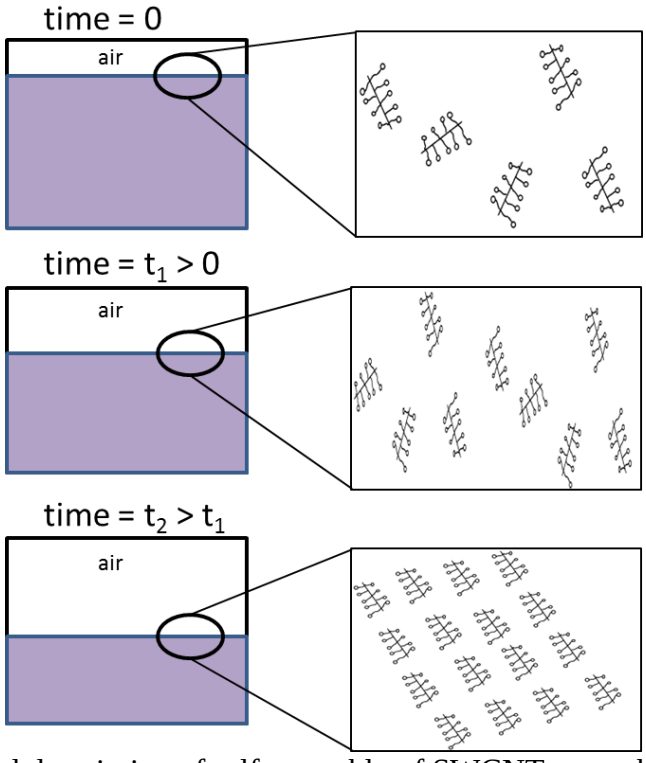

Figure 3.3 Graphical description of self-assembly of SWCNTs near the air-water surface during the evaporative deposition process.

In the work of Shastry et al,[78] large area SWCNT thin films were fabricated using an evaporation driven self-assembly. The authors explain the deposition of SWCNT/SDS complexes, on the vertically inserted substrate, by the combination of frictional and capillary forces between the substrate and the suspended particles. The frictional forces pin the particles in place, while the capillary forces can lead to de-pinning of the particles. The competition between diffusional forces and the accelerated evaporation at the contact line yields dense stripes of SWCNTs. Thus, the formation of stripes of SWCNTs on the surface is governed by the concentration of SWCNT/SDS complexes and the surface tension of the solution. In other words, increasing the concentration of SWCNT/SDS increases the friction between the substrate and the solution. On the other hand, increasing the concentration of SDS lowers the surface tension of the solution and requiring less force to de-pin the contact line.[78]

In the following experiments, standard microscope glass substrates are cut to the desired size and cleaned with acetone and DI water. The substrates are left to dry before being placed vertically in a solution of separated semiconducting SWCNTs, as shown in Figure 3.4. The solutions used here contain either a mixture of surfactants, SDS and SC, or a mixture of SDS with NaCl. The evaporation temperature in all experiments is kept at 70 °C.

Figure 3.4 Glass substrates in a solution of sc-SWCNTs/SDS/SC.

In Figure 3.4, two sc-SWCNT films are simultaneously deposited on the two substrates shown. In the solution, containing a mixture of SDS and SC, the edge of the deposited film is defined by the meniscus formed on the substrate. This in turn is governed by the surface tension of the solution. As the water starts to evaporate, stripes defining the edge of the film are visually observed. This indicates that a thick region of multiple layers of sc-SWCNTs are depositing on the substrate. The high thickness of the deposited film is attributed to the high concentration of SWCNT/surfactant in the starting solution as well as the evaporation rate.

Since the contact line is dropping with a velocity greater than the diffusion velocity of SWCNTs, they remain trapped near the surface of the solution forming the first layer of SWCNT/surfactant. If this layer is not adsorbed to the substrate, multiple layers can form beneath it. The layers formed near the surface are not in a bundled state due to the repulsive forces between micelles on the SWCNTs. This is evident by the absence of observable aggregation on the surface of the solution and the prepared films

(Figure 3.5). However, one must also consider that the elevated temperatures used in the evaporation process can impact the micelle structure around SWCNTs. If it is assumed that a behavior similar to that of pure surfactant micelles in water is taking place, then it is possible to hypothesize that the micelles surrounding SWCNTs are undergoing a transition to a lower aggregation state, meaning less SDS are adsorbed to the surface of a SWCNT.[83] This indicates a need to avoid extreme evaporation temperatures that may result in pre-aggregation rather than the desired structured deposition.

Figure 3.5 Semi-transparent SWCNT film on glass.

To investigate the morphology of SWCNTs on the film shown in Figure 3.5, absorption spectroscopy provides a simple approach to test the individualization of SWCNTs in the solid state. This can only be applied to sc-SWCNTs since they display distinct (*n*,*m*) transitions in the E_{11} and E_{22} regions. In m-SWCNTs the various (*n*,*m*) absorption peaks are detectable as broad bands, and since multiple peaks are significantly overlapping with each other, it is difficult to judge the extent of their aggregation or individualization. In the following absorption spectrum, only the sc-SWCNT E_{22} region

between 450 – 800 nm is investigated due to the detection limitations of the instrument used (Shimadzu UV-2401).

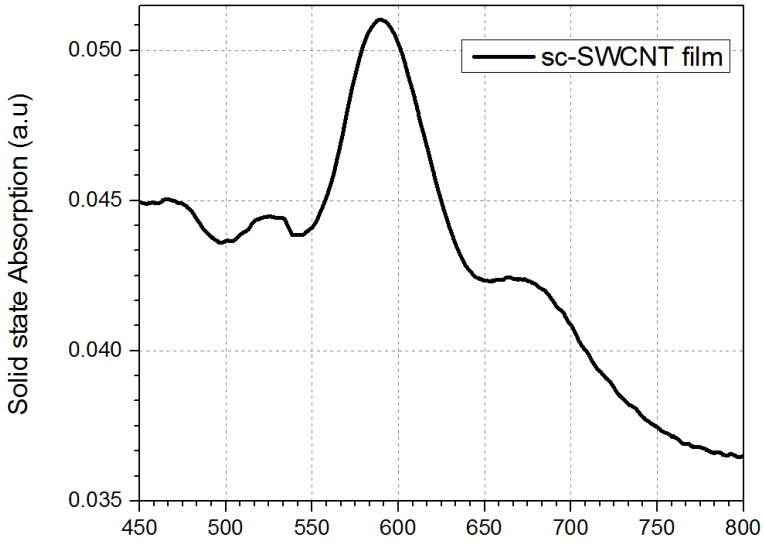

Figure 3.6 Optical absorption of sc-SWCNT thin film on glass substrate.

Figure 3.6 shows the absorption of SWCNTs in the solid state. The results reduce the possibility of aggregation of the layers of SWCNTs in the solid state. This is justified by the ability to see distinct (*n*,*m*) transitions instead of one broad peak, for instance the primary (6,5) peak at ~580 nm.

There are many reasonable explanations for the formation of cracks in the films prepared with the same procedure (sc-SWCNT/SDS/SC) shown in Figure 3.5. One being the presence of free surfactant micelles that can affect the stacking near the interface, resulting in imperfections in the deposited film. Another possible explanation is the presence of mechanical vibrations in the work station affecting the contact line. When the same experimental procedure is repeated for the sc-SWCNT suspensions separated with NaCl, no observable stripes are shown on the substrate. More interesting is that the SWCNTs started to aggregate in the suspension at an early stage.

In another experiment to test the effects of surfactant concentration on deposition, a sc-SWCNT suspension separated from the same initial concentration (2 mg in 2 wt% SDS, eluted with 1 wt% SC) is diluted with 10 mL of 1 wt% SC and sonicated for 30 minutes at a power of ~12 W before inserting the glass substrate, as shown in Figure 3.7a. At the same evaporation temperature (70 °C), SWCNT deposition did not start at the initial interface line. Moreover, as evaporation continues, SWCNTs displayed observable aggregation on the substrate as shown in Figure 3.7b.

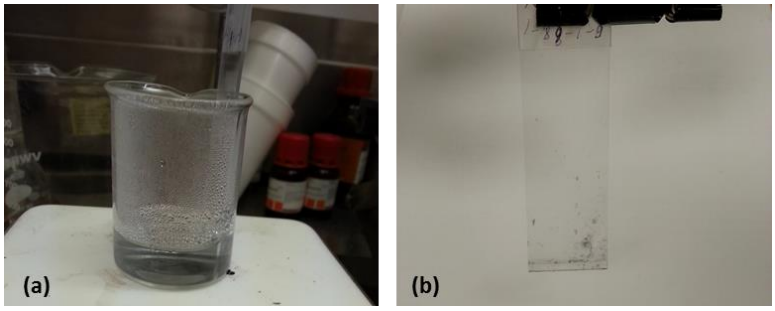

Figure 3.7 (a) Glass substrate in a dilute solution of sc-SWCNT/SC, and **(b)** aggregation of SWCNTs on the substrate.

The aggregation of SWCNTs on the substrate when deposited from either a suspension of high concentration of surfactant or salt is best described by the increase in the diffusivity of SWCNT/surfactant complexes in the medium. This is due to the decrease in the viscosity of the suspension when surfactants or salts are present. These observations may be described using the Stokes-Einstein equation for translational diffusion. Following the assumption of Hobbie et al.[84] that SWCNT/SDS structures can be modeled as rigid rods, the equation is written as:

$$D = \frac{kT\ 2\ \ln\left(\frac{L}{d}\right) - \gamma}{6\ \pi\ \mu\ L} \qquad (3.1)$$

Where D is the mean diffusion coefficient of SWCNTs, k is the Boltzmann constant, T is the temperature (343 K), μ is the viscosity of the solution, L is the length of the SWCNT,

d is the diameter of the supramolecular (SWCNT/SDS) complex, and γ is a correction factor.[85] The mean diameter of the SWCNT sample is 0.78 ± 0.16 nm, with an aspect ratio (*L*/*d*) of ~1000 (SouthWest Nanotechnologies, SG65i, Appendix A1).

In the deposition experiments where SWCNTs are self-assembled from a suspension of SDS/SC, when the concentration of SC is increased, the viscosity term (μ) in equation 3.1 is decreased, resulting in an enhanced diffusivity (*D*) of the SWCNT/SDS complex in the medium. Thus, SWCNTs can diffuse to the low concentration region faster than the drop rate of the air/suspension interface.

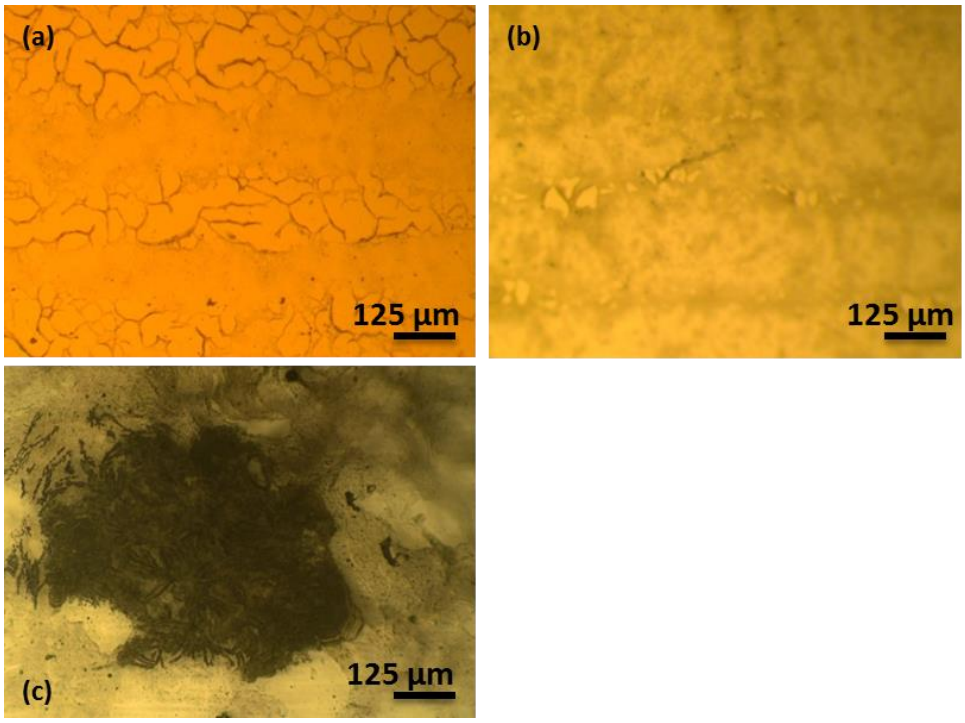

Figure 3.8 SWCNTs/surfactant on glass substrates deposited from **(a)** higher viscosity solution, **(b)** solutions having high concentration of SWCNTs, and **(c)** solutions of lower viscosity.

A closer look at the deposited films using optical microscopy (Figure 3.8) shows the bulk morphology on the micrometer scale. In the case when separated sc-SWCNTs are deposited from a solution of SWCNTs/SDS/SC, the deposited film in Figure 3.8a shows non-uniform stripes of SWCNT/surfactant with gaps having widths of ~100 µm. In

the films deposited from unseparated SWCNTs/SDS, the film appears to be continuous with few visible imperfections (Figure 3.8b). In the experiments where SWCNTs are deposited from solutions of high surfactant concentration (i.e. low viscosity), a closer look shows large aggregates of SWCNTs/surfactant on the glass surface. These observations are in agreement with expectations based on the application of the Stokes-Einstein equation (3.1), the rigid rod model from Hobbie et al., and illustrated previously in Figure 3.3.

3.3 Conclusions

For many applications of SWCNTs it is helpful to have schemes for their deposition as thin films. While bulk, as-produced SWCNTs have been used in early efforts, desired benefits in optoelectronics, for instance, require more refined SWCNT materials like those resulting from separations processes. Since these processes typically yield SWCNTs wrapped in surfactants, finding methods to remove the surfactant prior to thin film deposition, or to deposit the SWCNT/surfactant complexes directly (to later remove the surfactant) are necessary.

In this chapter, it was shown that surfactants can be removed readily by an aggregation/washing process that included addition of simple organic solvents (methanol or acetone) to the SWCNT/surfactant suspensions followed by low-speed centrifugation, SWCNT material collection, and brief colloidal suspension in for instance another organic solvent like acetone or DMF for spin coating. It was also shown that direct evaporative deposition from a SWCNT/surfactant aqueous suspension can yield ordered thin films on a micron to millimeter scale. Earlier literature descriptions of this process could not properly describe or account for deposition failures. By treating the

SWCNT/surfactant complex as a rigid rod, this diffusion controlled process, well described by the Stokes-Einstein equation, can be purposefully modified by temperature, counter-ion addition, and/or surfactant concentration. Such demonstrations now provide a more comprehensive understanding of the process of SWCNT self-assembly which can open the door to a wide range of SWCNT applications.

CHAPTER 4: CONCLUSIONS AND REMARKS

4.1 Summary of Current Results

Most work with SWCNT gel-based chromatography separations rely on employing either different concentrations of one surfactant or introducing cosurfactants. In both cases, surfactant monomers tend to adsorb to the exposed regions of SWCNTs altering their affinity toward the gel medium (typically a modified allyl dextran).

In Chapter 2 of this work, a simple and cost effective separation method was presented. By introducing alkali metal ionic salts, the interaction between adsorbed sc-SWCNTs and the gel medium is disturbed leading to the desired elution. The effect of changing the size of the metal cation is shown to affect the wrapping of SDS monomers around SWCNTs. At similar concentrations of salt, smaller cations (Li^+) yielded little sc-SWCNT elution while larger cations (e.g. K^+) were found to cause aggregation. This was explained by the difference in hydration, that is smaller cations are surrounded by a larger number of water molecules making it difficult to approach surfactant headgroups. By testing salts having different anions, we demonstrate that the elution from gel is mainly driven by the positively charged metal ions.

Absorption spectroscopy was used throughout this thesis to analyze the difference between samples eluted with different salt solutions. The samples obtained following the addition of salts displayed higher degrees of SWCNT individualization in the collected fractions. These findings support the work in the literature describing the effect on the separation process related to the SDS packing density around different SWCNTs. In the experiments utilizing various metal ionic salts, it is demonstrated that the separation is only affected by the wrapping of SDS around SWCNTs.

To fully understand the separation of SWCNTs, iterative peak fitting of SWCNT absorption spectra, collected following the addition of different concentrations of NaCl, is employed. A small window in the E_{11} region is analyzed (830 – 1100 nm). Using Voigt basis functions and least-squares fitting, the relative concentrations of several (*n,m*) species are calculated at the different [NaCl] levels. The results of the fitting shows how different (*n,m*) SWCNTs require different salt concentrations to reach an aggregation stage. Namely, larger diameter species such as (10,2) tend to aggregate at lower concentrations of NaCl.

In Chapter 3, different methods for SWCNT deposition on glass substrates are presented. In section 3.1, separated SWCNTs are first stripped from the surfactant wrapping them by a repetitive addition of an organic solvent, such as methanol or acetone, followed by mild centrifugation at 1500 RPM, and then resuspension in a volatile solvent. SWCNT suspensions prepared following this procedure were stable for 3-10 minutes depending on the concentration of SWCNTs. These suspension could then be readily spin coated onto a substrate. In section 3.2, separated SWCNTs are deposited directly on glass substrates via vertical deposition from an evaporated aqueous suspension. A novel approach to explain the mechanism of deposition is presented, wherein, the results are explained by combining Tsyboulski's diffusion dynamics,[86] Hobbie's self assembly method[84] and Shastry's mechanistic model.[78] The Stokes-Einstein equation of diffusion for cylindrical rods is used to understand SWCNTs self-assembly near the air/suspension interface. The competition between drop rate of the interface line and the diffusion rate of SWCNT/SDS complexes is found to be responsible for SWCNT

concentration near the interface. The presence of Coulombic repulsion between surfactant micelles is found to drive the self-assembly of SWCNTs near the interface.

4.2 Suggestions for Future Work

In section 2.2, the effect of introducing salts to SWCNT/SDS suspensions was described. However, one can test a wider range of salts (including CsCl, $MgCl_2$, $CaCl_2$, and NH_4Cl) to solidify the effect of larger salt cations and consider divalent or trivalent metal ions in the eluting solution on the separated SWCNT/SDS fractions. These experiments should also provide insight on whether ionic activity is more important than ion size. In a manner similar to that explained in section 3.1, it is also possible to test whether organic solvents such ethanol, methanol, or acetone can cause SWCNTs to be eluted from a gel medium. This will help create a ready to be used SWCNT ink for spray or spin coating applications.

Another direction that might allow scientists and engineers to better understand the adsorption interactions of SWCNT/surfactant complexes is to consider studying the thermodynamics of micelle formation on SWCNTs with different electronic character. This could be done using calorimetric experiments observing micelle formation and disintegration as a function of temperature. This will allow the determination of the enthalpy and entropy of micelle formation on both metallic and semiconducting SWCNTs. Initially, one can start by looking at previous experimental work dealing with pure SDS micelles in water.

In section 3.2, the effect of controlling the hydrophobicity of the substrate was not investigated. A possible method might include plasma etching of the glass substrate which will reduce the hydrophobicity of the substrate. Moreover, by tagging the

nanotubes with fluorescent dye, one might be able to observe the morphology of SWCNT films using confocal fluorescence microscopy.

REFERENCES

1. Dresselhaus, M. S.; Dresselhaus, G.; Avouris, Ph. *Carbon Nanotubes: Synthesis, Structure, Properties, and Applications;* Springer-Verlag: New York, 2001; Vol. 80.

2. Reich, S.; Janina, J.; Thomsen, C. *Carbon Nanotubes: Basic Concepts and Physical Properties;* Wiley: New York, 2004.

3. Ouyang, M.; Huang, J.-L.; Lieber, C. M. Fundamental electronic properties and applications of single-walled carbon nanotubes. *Acc. Chem. Res.* **2002,** *35*, 1018-1025.

4. Saito, R.; Dresselhaus, G.; Dresselhaus, M. S. *Physical Properties of Carbon Nanotubes;* Imperial College Press: London, 1998.

5. Saito, R.; Fujita, M.; Dresselhaus, G.; Dresselhaus, M. S. Electronic structure of graphene tubules based on C_{60}. *Physical Review B* **1992,** *46*, 1804-1811.

6. Bachilo, S. M.; Balzano, L.; Herrera, J. E.; Pompeo, F.; Resasco, D. E.; Weisman, R. B. Narrow (n,m)-distribution of single-walled carbon nanotubes grown using a solid supported catalyst. *J. Am. Chem. Soc.* **2003,** *125*, 11186-11187.

7. Lolli, G.; Zhang, L.; Balzano, L.; Sakulchaicharoen, N.; Tan, Y.; Resasco, D. E. Tailoring (n,m) Structure of Single-Walled Carbon Nanotubes by Modifying Reaction Conditions and the Nature of the Support of CoMo Catalysts. *J. Phys. Chem. B* **2006,** *110* (5), 2108-2115.

8. Dai, H.; Rinzler, A. G.; Nikolaev, P.; Thess, A.; Colbert, D. T.; Smalley, R. E. Single-wall nanotubes produced by metal-catalyzed disproportionation of carbon monoxide. *Chem. Phys. Lett.* **1996,** *260*, 471-475.

9. Fan, X. F.; Buczko, R.; Puretzky, A.; Geohegan, D. B.; Howe, J. Y.; Pantelides, S. T.; Pennycook, S. J. Nucleation of single-walled carbon nanotubes. *Phys. Rev. Lett.* **2003,** *90* (14), 145501-1-145501-4.

10. Bayer, B. C.; Hofmann, S.; Castellarin-Cudia, C.; Blume, R.; Baehtz, C.; Esconjauregui, S.; Wirth, C. T.; Oliver, R. A.; Ducati, C.; Knop-Gericke, A.; Schlogl, R.; Goldoni, A.; Cepek, C.; Robertson, J. Support-Catalyst-Gas Interactions during Carbon Nanotube Growth on Metallic Ta Films. *J. Phys. Chem. C* **2011,** *115* (11), 4359-4369.

11. Kitiyanan, B.; Alvarez, W. E.; Harwell, J. H.; Resasco, D. E. Controlled production of single-wall carbon nanotubes by catalytic decomposition of CO on bimetallic Co-Mo catalysts. *Chem. Phys. Lett.* **2000,** *317*, 497-503.

12. Iijima, S. Helical microtubules of graphitic carbon. *Nature* **1991,** *354*, 56-58.

13. Grossiord, N.; Loos, J.; Regev, O.; Koning, C. E. Toolbox for dispersing carbon nanotubes into polymers to get conductive nanocomposites. *Chem. Mater.* **2006,** *18* (5), 1089-1099.

14. Yu, M. F.; Files, B. S.; Arepalli, S.; Ruoff, R. S. Tensile Loading of Ropes of Single Wall Carbon Nanotubes and their Mechanical Properties. *Phys. Rev. Lett.* **2000,** *84* (24), 5552-1-5552-4.

15. Fanchini, G.; Miller, S.; Parekh, B. B.; Chhowalla, M. Optical Anisotropy in Single-Walled Carbon Nanotube Thin Films: Implications for Transparent and Conducting Electrodes in Organic Photovoltaics. *Nano Lett.* **2008**.

16. Liu, P.; Lee, S. H.; Yan, Y. F.; Gennett, T.; Landi, B. J.; Dillon, A. C.; Heben, M. J. Electrochemical transformation of SWNT/Nafion composites. *Electrochemical and Solid State Letters* **2004,** *7* (11), A421-A424.

17. Franklin, N. R.; Wang, Q.; Tombler, T. W.; Javey, A.; Shim, M.; Dai, H. Integration of suspended carbon nanotube arrays into electronic devices and electromechanical systems. *Appl. Phys. Lett.* **2002,** *81* (5), 913-915.

18. Zhu, H.; Hu, L.; Cumings, J.; Huang, J.; Chen, Y.; Preston, C.; Rohrbach, K. Highly Transparent and Flexible Nanopaper Transistor. *ACS Nano* **2013,** *7* (3), 2106-2113.

19. Blom, P. W. M.; Mihailetchi, V. D.; Koster, L. J. A.; Markov, D. E. Device Physics of Polymer:Fullerene Bulk Heterojunction Solar Cells. *Advanced Materials* **2007,** *19* (12), 1551-1556.

20. Bernardi, M.; Lohrman, J.; Kumar, P. V.; Kirkeminde, A.; Ferralis, N.; Grossman, J. C.; Ren, S. Nanocarbon-Based photovoltaics. *ACS Nano* **2012,** *6* (10), 8896-8903.

21. Ren, S.; Bernardi, M.; Lunt, R. R.; Bulovic, V.; Grossman, J. C.; Gradecak, S. Toward efficient carbon nanotube/P3HT solar cells: active layer morphology, electrical, and optical properties. *Nano Lett.* **2011,** *11* (12), 5316-5321.

22. Sato, Y.; Yanagi, K.; Miyata, Y.; Suenaga, K.; Kataura, H.; Iijima, S. Chiral-Angle Distribution for Separated Single-Walled Carbon Nanotubes. *Nano Lett.* **2008,** *8* (10), 3151-3154.

23. Rocha, J.-D. R.; Bachilo, S. M.; Ghosh, S.; Arepalli, S.; Weisman, R. B. Efficient Spectrofluorimetric Analysis of Single-Walled Carbon Nanotube Samples. *Anal. Chem.* **2011,** *83* (19), 7431-7437.

24. Tsyboulski, D.; Rocha, J.-D. R.; Bachilo, S. M.; Cognet, L.; Weisman, R. B. Structure-dependent fluorescence efficiencies of individual single-walled carbon nanotubes. *Nano Lett.* **2007,** *7*, 3080-3085.

25. Carlson, L. J.; Krauss, T. D. Photophysics of Individual Single-Walled Carbon Nanotubes. *Acc. Chem. Res.* **2008,** *41* (2), 235-243.

26. Lian, Y. F.; Maeda, Y.; Wakahara, T.; Akasaka, T.; Kazaoui, S.; Minami, N.; Choi, N.; Tokumoto, H. Assignment of the fine structure in the optical absorption spectra of soluble single-walled carbon nanotubes. *J. Phys. Chem. B* **2003,** *107* (44), 12082-12087.

27. Bachilo, S. M.; Strano, M. S.; Kittrell, C.; Hauge, R. H.; Smalley, R. E.; Weisman, R. B. Structure-assigned optical spectra of single-walled carbon nanotubes. *Science* **2002,** *298* (5602), 2361-2366.

28. Arnold, M. S.; Stupp, S. I.; Hersam, M. C. Enrichment of single-walled carbon nanotubes by diameter in density gradients. *Nano Lett.* **2005,** *5* (4), 713-718.

29. Claudia Backes *Noncovalent Functionalization of Carbon Nanotubes;* 1st ed.; Springer Berlin - Heidelberg: Berlin, Germany, 2012.

30. Arnold, M. S.; Green, A. A.; Hulvat, J. F.; Stupp, S. I.; Hersam, M. C. Sorting carbon nanotubes by electronic structure using density differentiation. *Nat. Nano.* **2006,** *1* (1), 60-65.

31. Strano, M. S.; Dyke, C. A.; Usrey, M. L.; Barone, P. W.; Allen, M. J.; Shan, H.; Kittrell, C.; Hauge, R. H.; Tour, J. M.; Smalley, R. E. Electronic structure control of single-waited carbon nanotube functionalization. *Science* **2003,** *301* (5639), 1519-1522.

32. Ellison, M. D.; Gasda, P. J. Functionalization of single-walled carbon nanotubes with 1,4-benzenediamine using a diazonium reaction. *J. Phys. Chem. C* **2008,** *112* (3), 738-740.

33. Krupke, R.; Hennrich, F.; von Lohneysen, H.; Kappes, M. M. Separation of metallic from semiconducting single-walled carbon nanotubes. *Science* **2003,** *301* (5631), 344-347.

34. Tanaka, T.; Liu, H. P.; Fujii, S.; Kataura, H. From metal/semiconductor separation to single-chirality separation of single-wall carbon nanotubes using gel. *Physica Status Solidi-Rapid Research Letters* **2011,** *5* (9), 301-306.

35. Hearst, J. E.; Lfft, J. B.; Vinograd, J. The effect of pressure on the buoyant behavior pf deoxyribonucleic acid and tobaco mosaic virus in a density gradient at equilibrium in the ultracentrifuge. *Proc. Natl. Acad. Sci.* **1961,** *47* (7), 1015-1025.

36. Arnold, M. S.; Green, A. A.; Hulvat, J. F.; Stupp, S. I.; Hersam, M. C. Sorting carbon nanotubes by electronic structure using density differentiation. *Nat. Nano.* **2006,** *1* (1), 60-65.

37. Tanaka, T.; Jin, H.; Miyata, Y.; Kataura, H. High yield separation of metallic and semiconducting single-wall carbon nanotubes by agarose gel electrophoresis. *Appl. Phys. Exp.* **2008,** *1*, 114001.

38. Miyata, Y.; Yanagi, K.; Maniwa, Y.; Kataura, H. Optical Evaluation of the Metal-to-Semiconductor Ratio of Single-Wall Carbon Nanotubes. *J. Phys. Chem. C* **2008,** *112* (34), 13187-13191.

39. Tummala, N. R.; Striolo, A. SDS Surfactants on Carbon Nanotubes: Aggregate Morphology. *ACS Nano* **2009,** *3* (3), 595-602.

40. Lin, S. C.; Blankschtein, D. Role of the Bile Salt Surfactant Sodium Cholate in Enhancing the Aqueous Dispersion Stability of Single-Walled Carbon Nanotubes: A Molecular Dynamics Simulation Study. *J. Phys. Chem. B* **2010,** *114* (47), 15616-15625.

41. Moshammer, K.; Hennrich, F.; Kappes, M. Selective suspension in aqueous sodium dodecyl sulfate according to electronic structure type allows simple separation of metallic from semiconducting single-walled carbon nanotubes. *Nano Res.* **2009,** *2* (8), 599-606.

42. Tulevski, G. S.; Franklin, A. D.; Afzali, A. High Purity Isolation and Quantification of Semiconducting Carbon Nanotubes via Column Chromatography. *ACS Nano* **2013,** *7* (4), 2971-2976.

43. Silvera-Batista, C. A.; Scott, D. C.; McLeod, S. M.; Ziegler, K. J. A Mechanistic Study of the Selective Retention of SDS-Suspended Single-Wall Carbon Nanotubes on Agarose Gels. *J. Phys. Chem. C* **2011,** *115* (19), 9361-9369.

44. Liu, H. P.; Nishide, D.; Tanaka, T.; Kataura, H. Large-scale single-chirality separation of single-wall carbon nanotubes by simple gel chromatography. *Nature Communications* **2011,** *2*, 309.

45. Hirano, A.; Tanaka, T.; Kataura, H. Thermodynamic Determination of the Metal/Semiconductor Separation of Carbon Nanotubes Using Hydrogels. *ACS Nano* **2012,** *6* (11), 10195-10205.

46. Tvrdy, K.; Jain, R. M.; Han, R.; Hilmer, A. J.; McNicholas, T. P.; Strano, M. S. A Kinetic Model for the Deterministic Prediction of Gel-Based Carbon Nanotube Separation. *ACS Nano* **2013,** *7* (2), 1779-1789.

47. Liu, H.; Tanaka, T.; Urabe, Y.; Kataura, H. High-Efficiency Single-Chirality Separation of Carbon Nanotubes Using Temperature-Controlled Gel Chromatography. *Nano Lett.* **2013,** *13* (5), 1996-2003.

48. Cheng, Q.; Debnath, S.; Gregan, E.; Byrne, H. J. Effect of Solvent Solubility Parameters on the Dispersion of Single-Walled Carbon Nanotubes. *J. Phys. Chem. C* **2008,** *112*, 20154-20158.

49. Sturzl, N.; Hennrich, F.; Lebedkin, S.; Kappes, M. M. Near Monochiral Single-Walled Carbon Nanotube Dispersions in Organic Solvents. *J. Phys. Chem. C* **2009,** *113* (33), 14628-14632.

50. Chen, J.; Hamon, M. A.; Hu, H.; Chen, Y.; Rao, A. M.; Eklund, P. C.; Haddon, R. C. Solution properties of single-walled carbon nanotubes. *Science* **1998,** *282*, 95-98.

51. Moore, V. C.; Strano, M. S.; Haroz, E. H.; Hauge, R. H.; Smalley, R. E. Individually suspended single-walled carbon nanotubes in various surfactants. *Nano Lett.* **2003,** *3*, 1379-1382.

52. Matarredona, O.; Rhoads, H.; Li, Z. R.; Harwell, J. H.; Balzano, L.; Resasco, D. E. Dispersion of single-walled carbon nanotubes in aqueous solutions of the anionic surfactant NaDDBS. *J. Phys. Chem. B* **2003,** *107* (48), 13357-13367.

53. Strano, M. S.; Moore, V. C.; Miller, M. k.; Allen, M. J.; Haroz, E. H.; Kittrell, C.; Hauge, R. H.; Smalley, R. E. The Role of Surfactant Adsorption during Ultrasonication in the Dispersion of Single-Walled Carbon Nanotubes. *Nanoscience and Nanotechnology* **2003,** *3*, 81-86.

54. Tan, Y.; Resasco, D. E. Dispersion of Single-Walled Carbon Nanotubes of Narrow Diameter Distribution. *J. Phys. Chem. B* **2005,** *109* (30), 14454-14460.

55. Wang, D.; Chen, L. W. Temperature and pH-responsive single-walled carbon nanotube dispersions. *Nano Lett.* **2007,** *7* (6), 1480-1484.

56. Hirano, A.; Tanaka, T.; Urabe, Y.; Kataura, H. pH- and Solute-Dependent Adsorption of Single-Wall Carbon Nanotubes onto Hydrogels: Mechanistic Insights into the Metal/Semiconductor Separation. *ACS Nano* **2013,** *7* (11), 10285-10295.

57. Jain, R. M.; Tvrdy, K.; Han, R.; Ulissi, Z. W.; Strano, M. S. Quantitative Theory of Adsorptive Separation for the Electronic Sorting of Single-Walled Carbon Nanotubes. *ACS Nano* **2014,** *8* (4), 3367-3379.

58. Bachilo, S. M.; Strano, M. S.; Kittrell, C.; Hauge, R. H.; Smalley, R. E.; Weisman, R. B. Structure-assigned optical spectra of single-walled carbon nanotubes. *Science* **2002,** *298*, 2361-2366.

59. Tanaka, T.; Jin, H.; Miyata, Y.; Fujii, S.; Suga, H.; Naitoh, Y.; Minari, T.; Miyadera, T.; Tsukagoshi, K.; Kataura, H. Simple and Scalable Gel-Based

Separation of Metallic and Semiconducting Carbon Nanotubes. *Nano Lett.* **2009,** *9* (4), 1497-1500.

60. Weisman, R. B.; Bachilo, S. M.; Strano, M. S.; Kittrell, C.; Hauge, R. H.; Smalley, R. E. (n,m)-assigned absorption and emission spectra of single-walled carbon nanotubes. *AIP Conf. Proc.* **2003,** *685*, 241-245.

61. Tanaka, T.; Jin, H.; Miyata, Y.; Fujii, S.; Nishide, D.; Kataura, H. Mass separation of metallic and semiconducting single-wall carbon nanotubes using agarose gel. *physica status solidi (b)* **2009,** *246* (11-12), 2490-2493.

62. Tummala, N. R.; Morrow, B. H.; Resasco, D. E.; Striolo, A. Stabilization of aqueous carbon nanotube dispersions using surfactants: insights from molecular dynamics simulations. *ACS Nano.* **2010,** *4* (12), 7193-7204.

63. Hayashi, S.; Ikeda, S. Micelle Size and Shape of Sodium Dodecyl Sulfate in Concentrated NaCl Solutions. *American Chemical Society* **1980,** *84* (7), 744-751.

64. Quina, F. H.; Nassar, P. M.; Bonilha, J. B. S.; Bales, B. L. Growth of sodium dodecyl sulfate micelles with detergent concentration. *J. Phys. Chem.* **1995,** *99* (46), 17028-17031.

65. Weisman, R. B.; Bachilo, S. M. Dependence of optical transition energies on structure for single-walled carbon nanotubes in aqueous suspension: an empirical Kataura plot. *Nano Lett.* **2003,** *3*, 1235-1238.

66. Ikeda, S.; yashi, S.; Toyoko, L. Rodlike Micelles of Sodium Dodecyl Sulfate in Concentrated Sodium Halide Solutions. *The Journal of Chemical Physics* **1981,** *85* (1), 106-112.

67. Nair, N.; Usrey, M. L.; Kim, W.; Braatz, R. D.; Strano, M. S. Estimation of the (n,m) Concentration Distribution of Single-Walled Carbon Nanotubes from Photoabsorption Spectra. *Anal. Chem.* **2006,** *78*, 7689-7696.

68. Avouris, P.; Freitag, M.; Perebeinos, V. Carbon-nanotube photonics and optoelectronics. *Nat. Photon.* **2008,** *2* (6), 341-350.

69. LeMieux, M. C.; Sok, S.; Roberts, M. E.; Opatkiewicz, J. P.; Liu, D.; Barman, S. N.; Patil, N.; Mitra, S.; Bao, Z. Solution assembly of organized carbon nanotube networks for thin-film transistors. *ACS Nano.* **2009,** *3* (12), 4089-4097.

70. Kaempgen, M.; Chan, C. K.; Ma, J.; Cui, Y.; Gruner, G. Printable Thin Film Supercapacitors Using Single-Walled Carbon Nanotubes. *Nano Lett.* **2009,** *9* (5), 1872-1876.

71. Saha, A.; Ghosh, S.; Weisman, R. B.; Marti, A. A. Films of Bare Single-Walled Carbon Nanotubes from Superacids with Tailored Electronic and Photoluminescence Properties. *ACS Nano* **2012,** *6* (6), 5727-5734.

72. Jo, J. W.; Jung, J. W.; Lee, J. U.; Jo, W. H. Fabrication of Highly Conductive and Transparent Thin Films from Single-Walled Carbon Nanotubes Using a New Non-ionic Surfactant via Spin Coating. *ACS Nano* **2010,** *4* (9), 5382-5388.

73. Huang, L. M.; Cui, X. D.; Dukovic, G.; O'Brien, S. P. Self-organizing high-density single-walled carbon nanotube arrays from surfactant suspensions. *Nanotechnology* **2004,** *15* (11), 1450-1454.

74. Park, S.; Vosguerichian, M.; Bao, Z. A. A review of fabrication and applications of carbon nanotube film-based flexible electronics. *Nanoscale* **2013,** *5* (5), 1727-1752.

75. Meitl, M. A.; Zhou, Y.; Gaur, A.; Jeon, S.; Usrey, M. L.; Strano, M. S.; Rogers, J. A. Solution Casting and Transfer Printing Single-Walled Carbon Nanotube Films. *Nano Lett.* **2004,** *4* (9), 1643-1647.

76. Cao, Q.; Rogers, J. A. Ultrathin Films of Single-Walled Carbon Nanotubes for Electronics and Sensors: A Review of Fundamental and Applied Aspects. *Advanced Materials* **2009,** *21* (1), 29-53.

77. Wu, Z. C.; Chen, Z. H.; Du, X.; Logan, J. M.; Sippel, J.; Nikolou, M.; Kamaras, K.; Reynolds, J. R.; Tanner, D. B.; Hebard, A. F.; Rinzler, A. G. Transparent, conductive carbon nanotube films. *Science* **2004,** *305* (5688), 1273-1276.

78. Shastry, T.; Seo, J. T.; Lopez, J. J.; Arnold, H. N.; Kelter, J. Z.; Sangwan, V. K.; Lauhon, L. J.; Hersam, M. C. Large-area, electronically monodisperse, aligned single-walled carbon nanotube thin films fabricated by evaporation-driven self-assembly. *Small* **2013,** *9* (1), 45-51.

79. Li, G.; Tang, J. X. Diffusion of actin filaments within a thin layer between two walls. *Phys. Rev. E* **2004,** *69*, 061921-1.

80. Duggal, R.; Pasquali, M. Dynamics of Individual Single-Walled Carbon Nanotubes inWater by Real-Time Visualization. *Phys. Rev. Lett.* **2006,** *96*, 246104-1-246104-4.

81. Bigioni, T. P.; Lin, X. M.; Nguyen, T. T.; Corwin, E. I.; Witten, T. A.; Jaeger, H. M. Kinetically driven self assembly of highly ordered nanoparticle monolayers. *Nat. Mater.* **2006,** *5* (4), 265-270.

82. Shimmin, R. G. Evaporation driven self-assembly as a route to photonic crystals. PhD Dissertation University of Illinios at Urbana-Champaign, ProQuest Dissertations And Theses, 2007.

83. Hammouda, B. Temperature Effect on the Nanostructure of SDS Micelles in Water. *Journal of Research of the National Institute of Standards and Technology* **2013,** *118*, 151-167.

84. Hobbie, E. K.; Fagan, J. A.; Becker, M. L.; Hudson, S. D.; Fakhri, N.; Pasquali, M. Self-Assembly of Ordered Nanowires in Biological Suspensions of Single-Wall Carbon Nanotubes. *ACS Nano* **2008,** *3* (1), 189-196.

85. Tsyboulski, D. A.; Bachilo, S. M.; Kolomeisky, A. B.; Weisman, R. B. Translational and Rotational Dynamics of Individual Single-Walled Carbon Nanotubes in Aqueous Suspension. *ACS Nano* **2008**.

86. Tsyboulski, D. A.; Bachilo, S.; kolomeisky, A. B.; Weisman, R. B. Translational and Rotational Dynamics of Individual Single-Walled Carbon Nanotubes in Aqueous Suspension. *ACS Nano* **2008,** *2* (9), 1770-1776.

APPENDIX

A1. SWeNT data sheets – SG65i

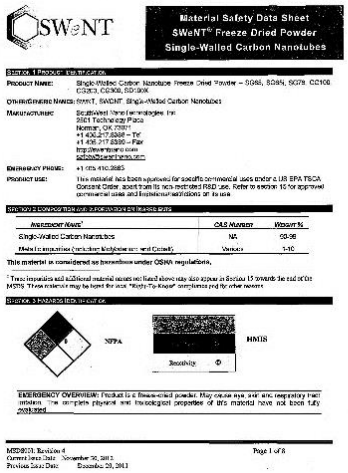

SWeNT

Material Safety Data Sheet
SWeNT® Freeze Dried Powder
Single-Walled Carbon Nanotubes

Section 1 Product Identification

Product Name: Single-Walled Carbon Nanotube Freeze Dried Powder – SG65, SG65i, SG76, CG100, CG300, CG100X

Chemical/Generic Name: pure f. SWCNT, Single-Walled Carbon Nanotubes

Manufacturer: SouthWest Nano Technologies Inc
3501 Technology Place
Norman, OK 73071
+1 405.217.6300 – Tel
+1 405.217.6330 – Fax
http://swnano.com
safety@swnano.com

Emergency Phone: +1 405.410.3665

Product Use: This material has been approved for specific commercial uses under a US EPA TSCA Consent Order, apart from its non-restricted R&D use. Refer to section 15 for approved commercial uses and limitations or its use.

Section 2 Composition and Information on Ingredients

Ingredient Name[1]	CAS Number	Weight %
Single-Walled Carbon Nanotubes	NA	90-96
Metal Impurities (including Molybdenum and Cobalt)	Various	1-10

This material is considered as hazardous under OSHA regulations.

[1] These impurities and additional material names not listed above may also appear in Section 15 towards the end of the MSDS. These substance may be listed the term "Kindly Tip Report" compliance and for other reasons.

Section 3 Hazards Identification

EMERGENCY OVERVIEW: Product is a freeze-dried powder. May cause eye, skin and, respiratory tract irritation. The complete physical and toxicological properties of this material have not been fully evaluated.

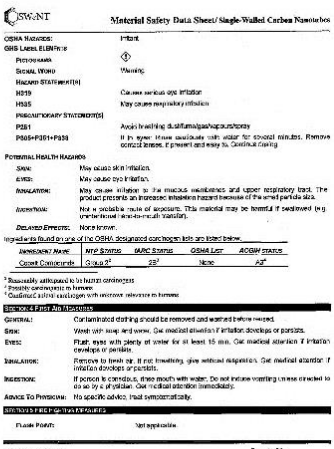

SWeNT **Material Safety Data Sheet/ Single-Walled Carbon Nanotubes**

OSHA Hazards: Irritant

GHS Label Elements

Pictograms

Signal Word: Warning

Hazard Statement(s)

H319 Causes serious eye irritation

H335 May causes respiratory irritation

Precautionary Statement(s)

P261 Avoid breathing dust/fume/gas/mist/vapors/spray

P305+P351+P338 If in eyes: Rinse cautiously with water for several minutes. Remove contact lenses, if present and easy to. Continue rinsing

Potential Health Hazards

Skin: May cause skin irritation.

Eyes: May cause eye irritation.

Inhalation: May cause irritation to the mucous membranes and upper respiratory tract. The product presents an inhalation hazard because of the small particle size.

Ingestion: Not a probable route of exposure. This material may be harmful if swallowed (e.g. unintentional hand-to-mouth transfer).

Delayed Effects: None known.

Ingredients found on one of the OSHA designated carcinogen lists are listed below.

Ingredient Name	NTP Status	IARC Status	OSHA List	ACGIH Status
Cobalt Compounds	Group 2[2]	2B[3]	None	A3[4]

[2] Reasonably anticipated to be human carcinogens
[3] Possibly carcinogenic to humans
[4] Confirmed animal carcinogen with unknown relevance to humans

Section 4 First Aid Measures

General: Contaminated clothing should be removed and washed before reused.

Skin: Wash with soap and water. Get medical attention if irritation develops or persists.

Eyes: Flush eyes with plenty of water for at least 15 min. Get medical attention if irritation develops or persists.

Inhalation: Remove to fresh air. If not breathing, give artificial respiration. Get medical attention if irritation develops or persists.

Ingestion: If person is conscious, rinse mouth with water. Do not induce vomiting unless directed to do so by a physician. Get medical attention immediately.

Advice To Physician: No specific advice. Treat symptomatically.

Section 5 Fire Fighting Measures

Flash Point: Not applicable.

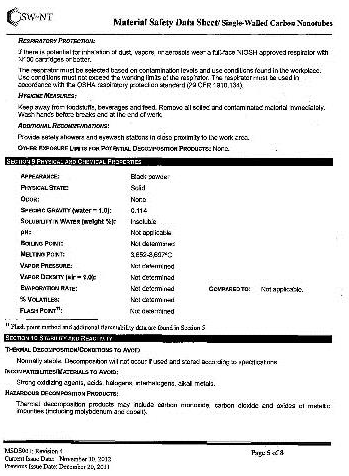

SWeNT **Material Safety Data Sheet/ Single-Walled Carbon Nanotubes**

Respiratory Protection:

If there is potential for inhalation of dust, vapors, or aerosols wear a full-face NIOSH approved respirator with N100 cartridges or better.

The respirator must be selected based on contamination levels and use conditions found in the workplace. Use conditions must not exceed the working limits of the respirator. The respirator must be used in accordance with the OSHA respiratory protection standard (29 CFR 1910.134).

Hygiene Measures:

Keep away from foodstuffs, beverages and feed. Remove all soiled and contaminated material immediately. Wash hands before breaks and at the end of work.

Additional Recommendations:

Provide safety showers and eyewash stations in close proximity to the work area.

On-site Exposure Limits for Personal Protective Products: None.

Section 9 Physical and Chemical Properties

Appearance:	Black powder		
Physical State:	Solid		
Odor:	None		
Specific Gravity (water = 1.0):	0.114		
Solubility in Water (weight %):	Insoluble		
pH:	Not applicable		
Boiling Point:	Not determined		
Melting Point:	3,650-3,697°C		
Vapor Pressure:	Not determined		
Vapor Density (air = 1.0):	Not determined		
Evaporation Rate:	Not determined	**Compared to:**	Not applicable.
% Volatiles:	Not determined		
Flash Point[1]:	Not determined		

[1] Flash point method and additional flammability data are found in Section 5.

Section 10 Stability and Reactivity

Thermal Decomposition/Conditions to Avoid:

Normally stable. Decomposition will not occur if used and stored according to specifications.

Incompatibilities/Materials to Avoid:

Strong oxidizing agents, acids, halogens, intercalants, alkali metals.

Hazardous Decomposition Products:

Thermal decomposition products may include carbon monoxide, carbon dioxide and oxides of metallic impurities (including molybdenum and cobalt).

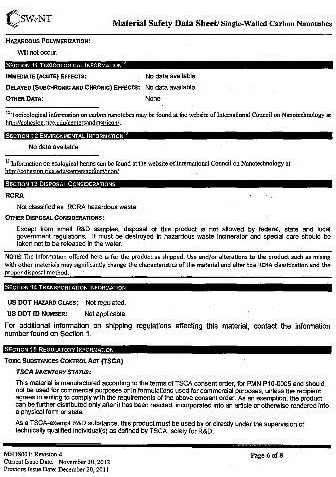

SWeNT **Material Safety Data Sheet/ Single-Walled Carbon Nanotubes**

Hazardous Polymerization:

Will not occur.

Section 11 Toxicological Information

Immediate (Acute) Effects: No data available.

Delayed (Subchronic and Chronic) Effects: No data available.

Other Data: None.

[1] Toxicological information on carbon nanotubes may be found at the website of International Council on Nanotechnology at http://cohesion.rice.edu/centersandinst/icon/.

Section 12 Ecological Information

No data available.

[1] Information on ecological hazards can be found at the website of International Council on Nanotechnology at http://cohesion.rice.edu/centersandinst/icon/.

Section 13 Disposal Considerations

RCRA:

Not classified as RCRA hazardous waste.

Other Disposal Considerations:

Except from small R&D samples, disposal of this product is not allowed by federal, state and local governmental regulations. It must be destroyed in hazardous waste incinerator and special care should be taken not to be released in the water.

NOTE: The information offered here is for the product as shipped. Use and/or alterations to the product such as mixing with other materials may significantly change the characteristics of the material and alter the RCRA classification and the proper disposal method.

Section 14 Transportation Information

US DOT Hazard Class: Not regulated.

US DOT ID Number: Not applicable.

For additional information on shipping regulations affecting this material, contact the information number found on Section 1.

Section 15 Regulatory Information

Toxic Substances Control Act (TSCA)

TSCA Inventory Status:

This material is manufactured according to the terms of TSCA consent order, for PMN P10-0305 and should not be used for commercial purposes or in manufacture, sold for commercial purposes, unless the recipient agrees in writing to comply with the requirements of the above consent order. As an exemption, the product can be further distributed only after it has been reacted in/incorporated into an article or otherwise rendered into a physical form or state.

As a TSCA-exempt R&D substance, this product must be used by or directly under the supervision of technically qualified individuals as defined by TSCA, solely for R&D.

SWeNT

Certificate of Analysis

Material *SG65i*

Lot Number *SG65i-L39*

Parameter	*Specification*	*Measured Value*	*Measurement Method*
P2B	*≥ 5.5*	*6.68(@981nm)*	*UV-vis-NIR Spectroscopy*
S2B	*>0.75*	*0.83*	*UV-vis-NIR Spectroscopy*
(6,5) content (% of sc tubes)	*≥ 40*	*41*	*NS2*
Semiconducting tube Content (%)	*≥ 95*	*TBD*	*UV-vis-NIR Spectroscopy*
Residual Mass (%)	*<5*	*3.35*	*TGA*
Average diameter (nm)	*0.78±0.1*	*0.78*	*NS2*
Raman Q = (1-D/G)	*≥ 0.97*	*0.975*	*NS2*
Relative Purity (T1%)	*≥93*	*99.17*	*TGA*

TBD = to be determined

Information certified by:

Philip Wallis.

Philip Wallis
Director, Quality & Technical Support
SouthWest Nanotechnologies

DISCLAIMER: THE INFORMATION HEREIN IS PROVIDED IN GOOD FAITH, AND IS BELIEVED TO BE ACCURATE. NO WARRANTY, EXPRESSED OR IMPLIED, IS MADE REGARDING THE ACCURACY OR COMPLETENESS OF THIS INFORMATION.

Optical Absorbance Spectrum – Lot# SG65i-L39

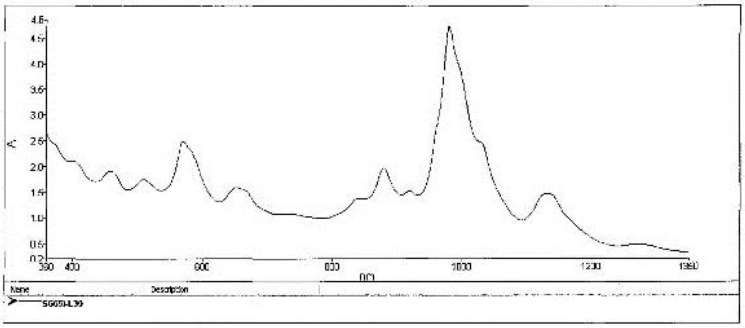

Thermogravimetric Analysis – Lot# SG65i-L39

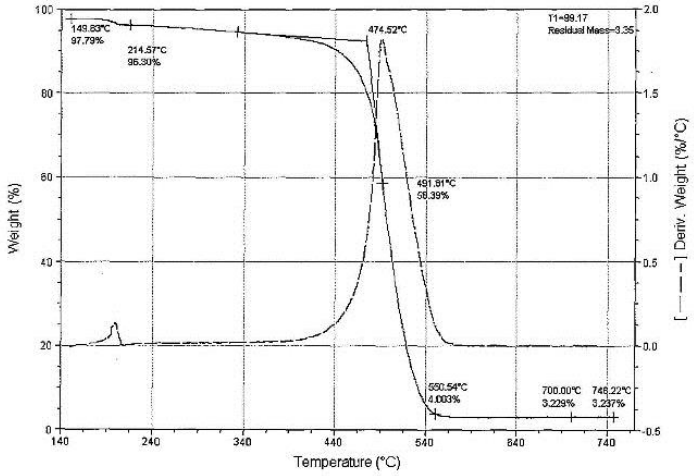

Raman Spectrum – Lot# SG65i-L39

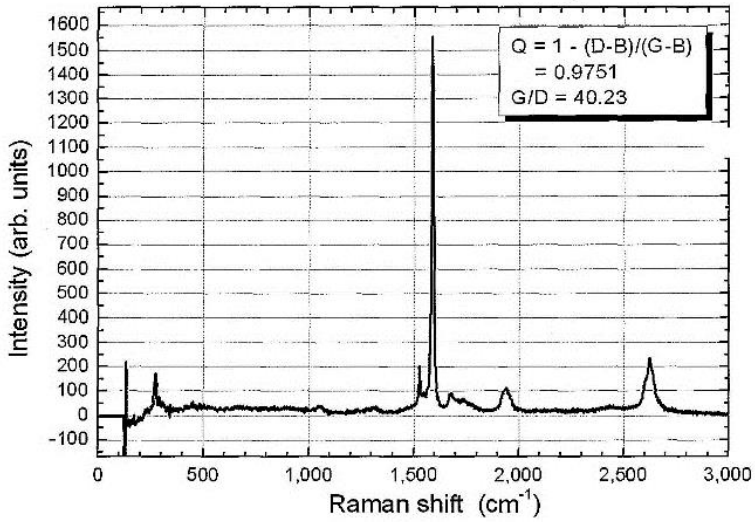

Chiral Distribution – Lot# SG65i-L39

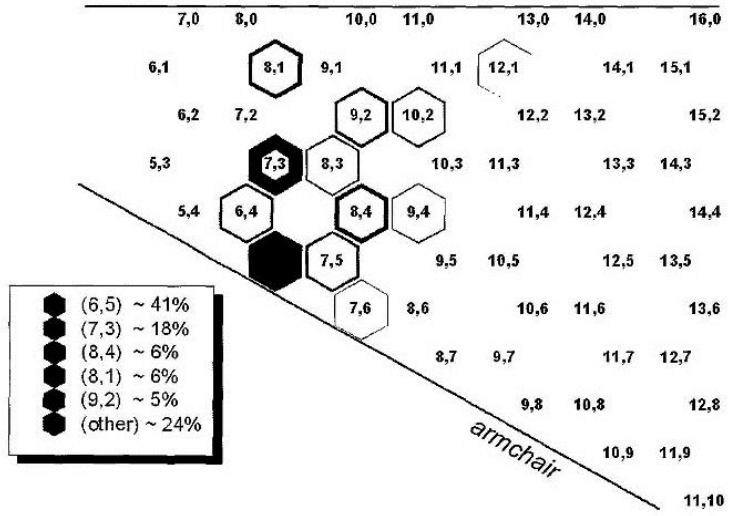

Diameter Distribution – Lot# SG65i-L39